



VirginiaTech
Invent the Future

**VIRGINIA POLYTECHNIC INSTITUTE
AND STATE UNIVERSITY**

The Charles E. Via, Jr. Department
of Civil and Environmental Engineering
Blacksburg, VA 24061

Structural Engineering and Materials

**EXPERIMENTAL EVALUATION OF A VEHICULAR ACCESS DOOR
SUBJECTED TO HURRICANE FORCE WIND PRESSURES**

by

Tian Gao

Graduate Research Assistant

Cristopher D. Moen, Ph.D., P.E.

Principal Investigator

Submitted to the:

Metal Building Manufacturers Association

1300 Sumner Ave

Cleveland, OH 44115-2851

Report No. CE/VPI-ST-09/03

November 2009

Acknowledgements

DBCI provided the use of their test facility in Douglasville, GA and supplied the rolling sheet doors used in the tests. Special thanks are extended to DBCI personnel, especially Mr. Bray Allen, who worked tirelessly to carry out the test plan. NCI Building Systems supplied the cold-formed framing members to assemble the typical metal building wall used in the test assembly. Mr. Jerry Hatch of NCI provided valuable guidance throughout the test program. Dr. Thomas Murray provided expertise as a testing consultant with respect to the project. Coordination with the sponsor was provided by Dr. Lee Shoemaker and Mr. Dan Walker of MBMA. Mr. Joe Hetzel of DASMA provided the important input of that group.

Table of Contents

Acknowledgements.....	1
1 Introduction.....	3
2 Testing Program.....	5
2.1 Rolling Sheet Doors Dimensions and Structural Details.....	5
2.2 Test Procedure.....	6
2.3 Data Acquisition.....	9
2.3.1 Strain Gauges.....	10
2.3.2 Out-of-Plane Steel Sheeting Deflections.....	11
2.3.3 Cold-Formed Steel Jamb Deflections.....	12
2.4 Test Results.....	13
2.4.1 Curtain Deflection vs. Pressure.....	13
2.4.2 Axial Force in Wind Lock vs. Pressure.....	18
2.4.3 Bending Moment vs. Pressure.....	20
2.5 Jamb Displacement vs. Pressure.....	23
3 Conclusions.....	24
4 Future Work.....	25
4.1 Jamb Flexibility.....	25
4.2 Finite Element Analysis.....	25
4.3 Simplified Mechanics-Based Prediction Models.....	26
4.4 Experimental Testing.....	26
References.....	27
Appendix A – Gauge Calibration Procedures.....	28
Appendix B – Strain Gauge Installation.....	30
Appendix C – Wind Lock Dimensions.....	31
Appendix D – DASMA Rolling Sheet Door Calculations.....	32
Appendix E – Wind Lock Strains.....	36

1 Introduction

Vehicular access doors are a commonly provided feature in metal building system applications. The most popular type of door is a rolling sheet door (Figure 1), where a cold-formed steel curtain spans between a door frame constructed of structural steel and/or cold-formed steel components. Steel restraints, called wind locks because of their ability to engage with the door frame in the case of a wind event, are riveted to the vertical edges of the curtain. The wind locks are free to move up and down under typical service conditions within a cold-formed steel guide attached to the door frame (Figure 2), although during an extreme wind event the wind locks engage with a wind bar also attached to the door jambs, preventing excessive out-of-plane deformation through a combination of metal-on-metal friction and the support provided by the door jamb.



Figure 1. Steel curtain rolling sheet door (view from the inside of a building)

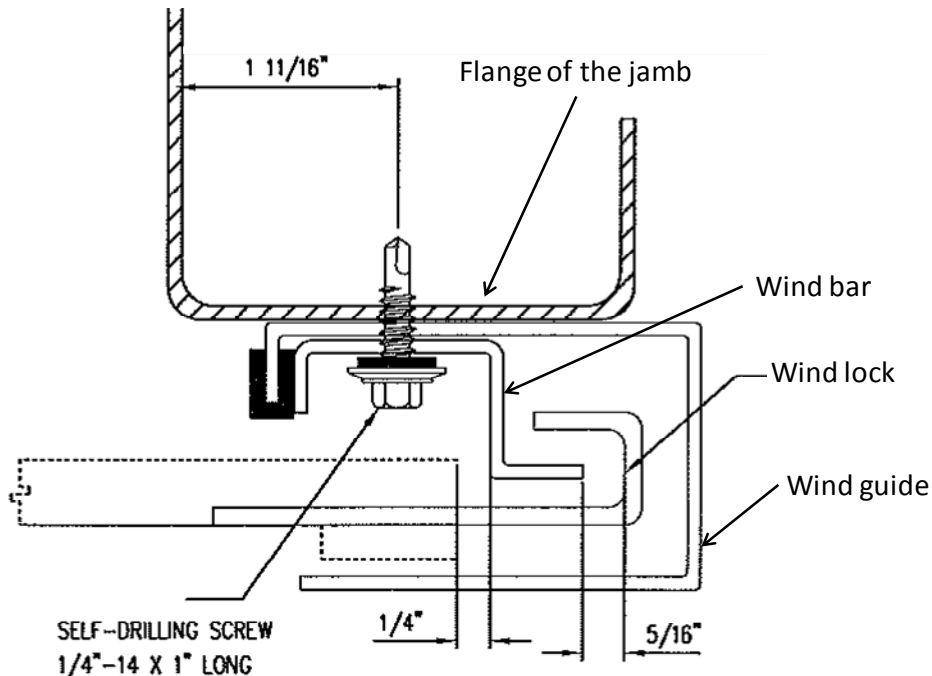


Figure 2. Typical details for a rolling sheet door provided with wind locks

The demand forces that develop in the wind lock, typically referred to as catenary forces in industry, are difficult to predict because of the complicated support conditions at the door-frame interface and the changing geometry of the steel curtain as the wind pressure is applied. For a stiffer door frame with masonry walls serving as jambs, the out-of-plane sheeting deformation will be small and the catenary design forces will be high, resulting in the potential for a connection failure at the wind lock or wind bar location. With a more flexible cold-formed steel door jamb, the catenary design forces will be lower but the out-of-plane deformation of the door will be larger, resulting in a potential failure mode where the wind locks slip off the wind bar.

The experimental study described herein was jointly sponsored by the Metal Building Manufacturers Association (MBMA) with the cooperation of the Door and Access Systems Manufacturers Association (DASMA) to study the behavior of a typical rolling sheet vehicular access door under a hurricane force wind pressure. The objectives are to quantify the structural behavior of a rolling sheet vehicular access door and the attached frame under both positive pressure (pushing the door into the building) and negative pressure (suction pulling the door away from the building), including the direct measurement of the catenary forces in the wind locks with strain gauges. The results will be used to optimize existing design methods for a rolling sheet vehicular access door and the supporting door frame.

2 Testing Program

2.1 Rolling Sheet Doors Dimensions and Structural Details

Two identical 10 ft. by 10 ft. steel curtain rolling sheet doors fitted with wind locks were tested in a custom pressure chamber at rolling sheet door manufacturing plant (Figure 1). The door frame component sizes and dimensions are provided in Figure 3, and Figure 5 provides pictures of the frame connections. Purlin bearing leg panels (i.e. PBR panels) with the dimensions described in Figure 4 were attached to the outside of the building frame with self-tapping machine screws.

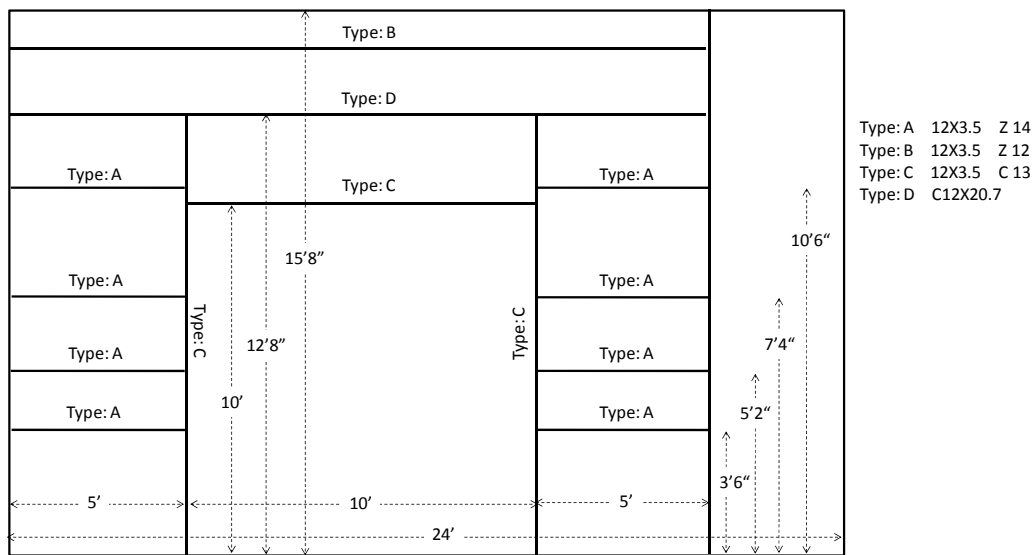


Figure 3. The dimension of the frame

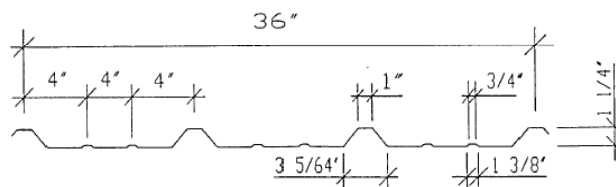


Figure 4 PBR panel cross-section (dimensions shown are for a 22 or 24 gauge panel)



Figure 5. Door frame details (picture taken from the inside of the building)

2.2 Test Procedure

Two rolling sheet doors were experimentally evaluated. Door #1 was loaded with a negative pressure (Door #1N, -80 psf max) followed by three separate positive pressure loading sequences (Door #1P-1, 60 psf max; Door #1P-2, 80 psf max; Door #1P-3, 140 psf max). Door #2 was loaded with a negative pressure (Door #2N, -80 psf max). The wall system supporting the door, including the cold-formed steel jambs and girts, were replaced before testing Door #2N. The pressure on the door was digitally recorded with a pressure transducer, and simultaneously monitored with a well-type manometer. For each test, the door was preloaded with a pressure of 10 psf and then released. The pressure was then reapplied in 10 psf increments until the maximum pressure output was reached from the blower or failure of the door occurred. Several unanticipated loading and unloading steps occurred during each of the four tests when the seal was lost in the vacuum chamber. The pressure time history for each test is provided in Figure 6 through Figure 10.

Note that even though the pressure transducer was observed to report constant pressure measurements at Virginia Tech (see Appendix A), during the tests the pressure transducer was observed to fluctuate by approximately ± 2 psf when holding a constant fan speed in the pressure chamber. The fluctuation was also observed in the manometer, and therefore it is hypothesized that the pressure variation was caused by harmonic fan speed variations.

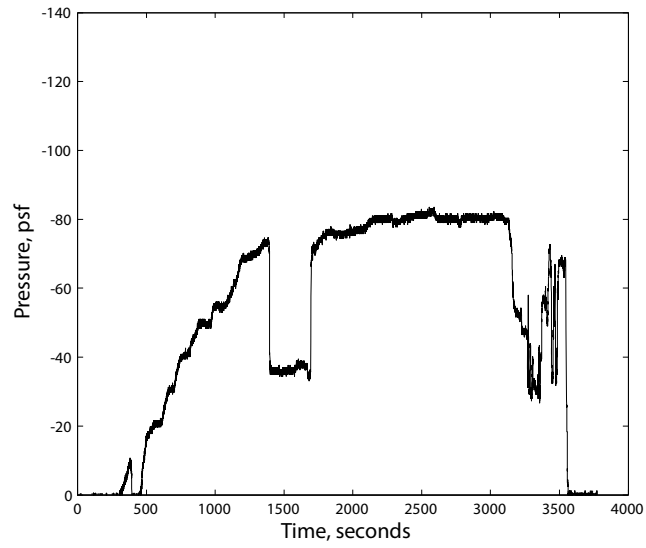


Figure 6. Pressure time history for Door #1N

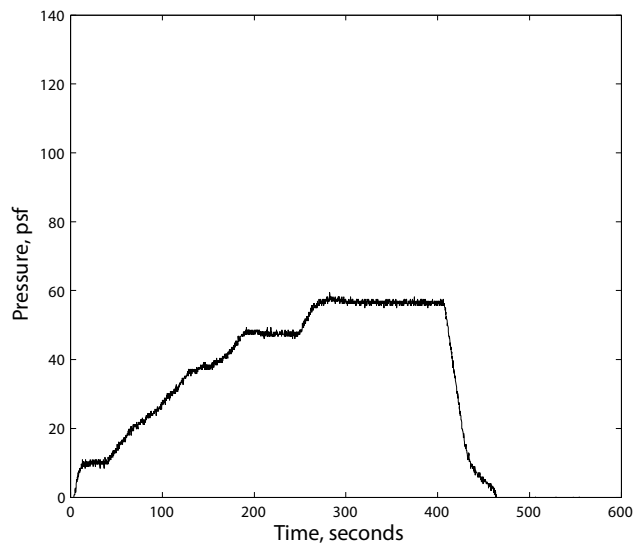


Figure 7. Pressure time history for Door #1P-1

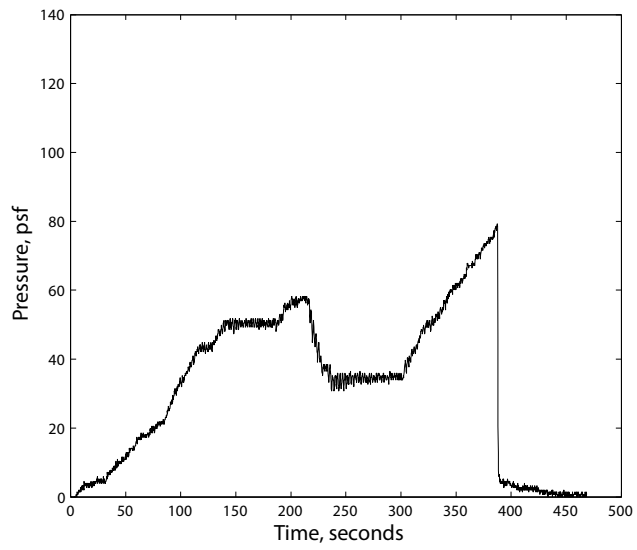


Figure 8. Pressure time history for Door #1P-2

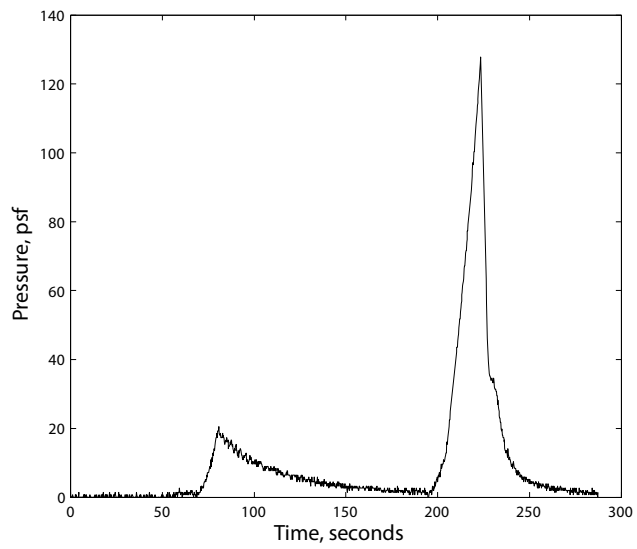


Figure 9. Pressure time history for Door #1P-3

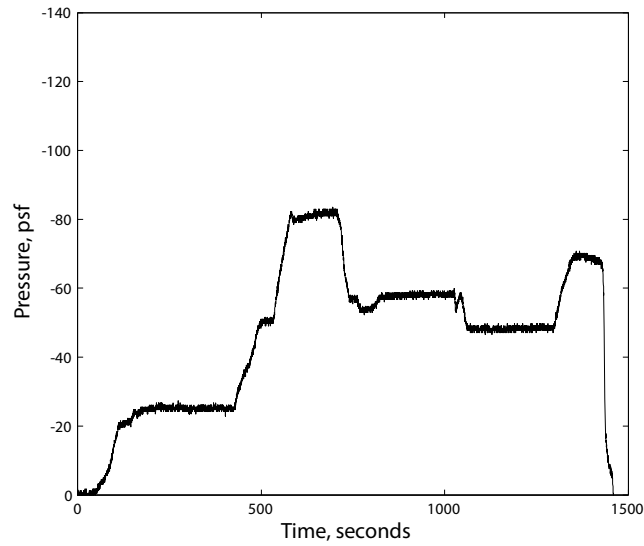


Figure 10. Pressure time history for Door #2N

2.3 Data Acquisition

A Vishay Micro-Measurements Model 5100B data acquisition system was used to digitally record 42 data channels at 5 points per second, including strain in the wind locks, deflection of the steel sheeting with wire potentiometers, deformation of the cold-formed steel door jambs with Linear Variable Differential Transformer (LVDTs), and chamber pressure with a pressure transducer during the test. All channels were zeroed immediately prior to testing. Figure 11 summarizes the gauge type and location, and the following sections provide details on their use and installation. Appendix A provides details on the gauge calibration procedures.

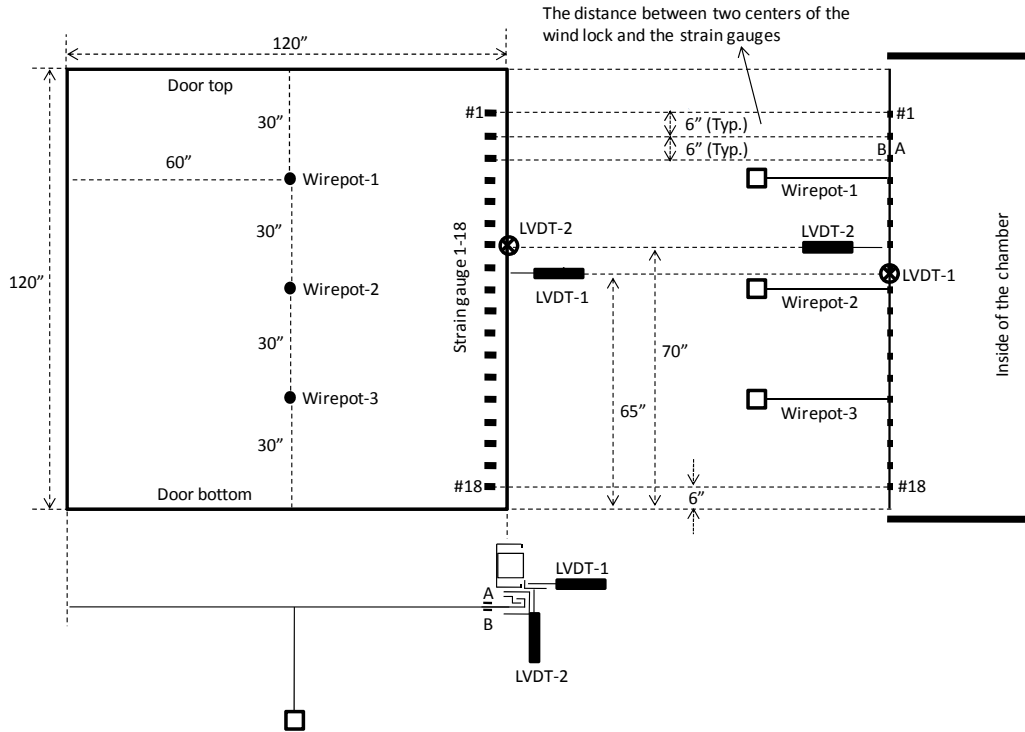


Figure 11. Wire pot, LVDT, and strain gauge locations

2.3.1 Strain Gauges

To accommodate the placement of strain gauges on the wind locks, the typical wind lock detail for a rolling sheet door was lengthened as shown in Figure 12. The modifications shifted the position of the riveted connection away from the wind guide, allowing the placement of the strain gauges (and associated wires) such that they did not interfere with the installation and operation of the door. The distance of the strain gauges from the riveted connection was set at approximately 2 times the width of the wind lock to ensure a uniform strain distribution in accordance with St. Venant's principle (Ugural and Fenster 2003).

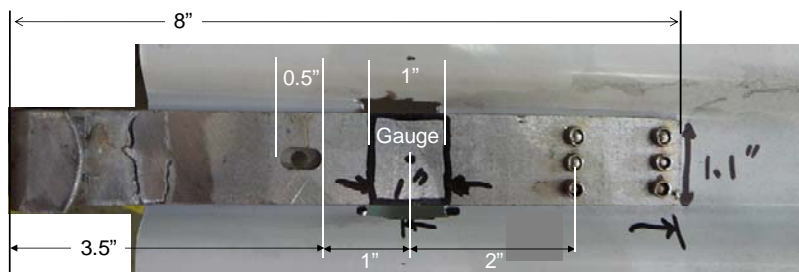


Figure 12. Lengthened wind lock and strain gauge location

A strain gauge was applied on each face of a wind lock. Strain gauge A faces towards the outside of the building, and Strain gauge B faces towards the inside of the building. (The strain gauge installation procedure is described in Appendix B.) Axial force, P (lbs), and moment, M (lb·in), in the wind lock at the gauge location are calculated with the formulas:

$$P = \left(\frac{\varepsilon_A + \varepsilon_B}{2} \right) EA, \quad (1)$$

and

$$M = \left(\frac{\varepsilon_A - \varepsilon_B}{2} \right) ES, \quad (2)$$

where ε_A and ε_B are the strains measured by gauge A and B respectively (note positive strain is tension), and A and S are the cross-sectional area and section modulus of the wind lock respectively. The modulus of elasticity for steel, E , is assumed as 30,000,000 psi. Eq. (1) and Eq. (2) are derived based on the assumption that the steel in the wind locks remained elastic at the strain gauge locations, which is consistent with the measured strains summarized in Appendix E. The average measured thickness and width for each wind lock are provided in Appendix C. Also note that $+P$ represents tension in the wind lock, and $+M$ represents a bending moment that creates tension on the face of the wind lock oriented toward the outside of the building.

2.3.2 Out-of-Plane Steel Sheeting Deflections

The steel sheeting deflection was recorded using wire potentiometers (wire pots) at 3 locations oriented along the vertical centerline of the door (see Figure 11). The wire pots were clamped to a steel column anchored to the concrete floor outside the pressure chamber as shown in Figure 13. The wire from each potentiometer was extended and attached to the door with sheet metal screws.



Figure 13. Wire pots were measure out-of-plane displacement

2.3.3 Cold-Formed Steel Jamb Deflections

LVDT-1 and LVDT-2 measured the in-plane displacement, a , and rotation of the jamb, b , respectively as pressure was applied to the door (Figure 14). LVDT-1 was attached to a horizontal girt (the location is described in Figure 11, also see Figure 15), and LVDT-2 was clamped on a steel frame isolated from the door system.

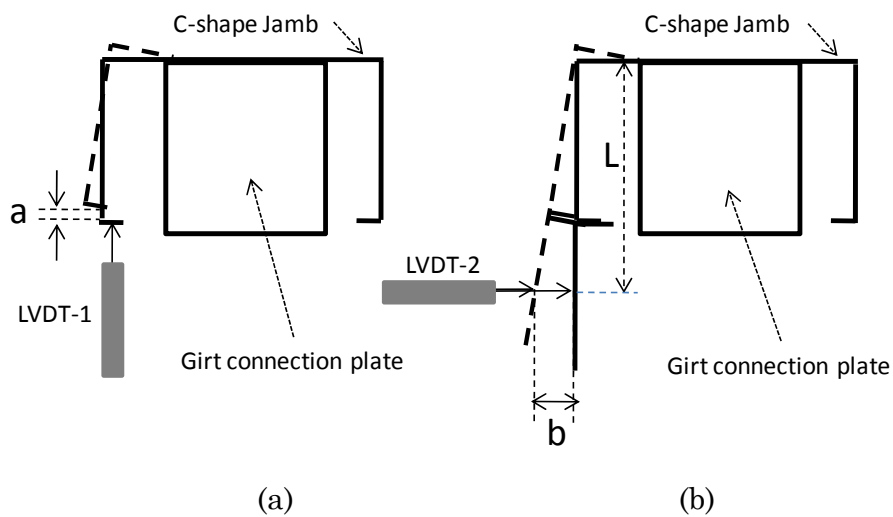


Figure 14. (a) In-plane displacement and (b) rotation of the jamb



Figure 15. LVDT-1 and LVDT-2 measure jamb displacements

2.4 Test Results

2.4.1 Curtain Deflection vs. Pressure

In both negative pressure tests (suction on the door pulling it out of the building) and positive pressure tests (pushing the door into the building), a bi-linear pressure-displacement curve was observed as shown in Figure 16 and Figure 17. (Note that pressure vs. displacement and displacement vs. pressure are provided for all figures to accommodate the preferences of the reader.) In the linear region (<10 psf or >10 psf), the wind locks are free to displace and are not restrained by the wind bar (see Figure 16 and Figure 17). As the pressure increases past ± 10 psf, the out-of-plane curtain deformation increases until the wind locks fully engage the wind bar at approximately ± 30 psf. The restraint of the door jamb limits further in-plane curtain deformation, which leads to an increase in stiffness denoted by the sharp change in slope in Figure 16 and Figure 17. The curtain demonstrates a higher unloading stiffness than loading stiffness (note the steeper descent in Figure 16 and Figure 17) which is hypothesized to occur from arching action shown in Figure 18 until the wind locks disengage from the wind bars.

For the negative pressure tests (Figure 16), the top and middle wire pots measured similar displacements at -60 psf (-11 in. for Door #1N top, -11 in. for Door #1N middle), while for the positive pressure test (Figure 17), there is a difference of 2 in. between the top and middle wire pots at 60 psf (10 in. for Door #1P-1 top, 12 in. for Door #1P-1 middle). It is hypothesized that this difference in displacements stems from the contribution of the barrel to the curtain deformation pattern as shown in Figure 19. The barrel limits the door deflection in a negative test, but has a minimal impact on curtain deflection for a positive pressure test. It is also noted that in all tests the slope of the pressure-displacement curve for the bottom wire pot is higher than the middle and the top, demonstrating the

increased stiffness provided by the angle fastened to the bottom of the curtain. (For Door #1P-3 which was loaded to 140 psf, the bottom angle was plastically deformed as shown in Figure 20.)

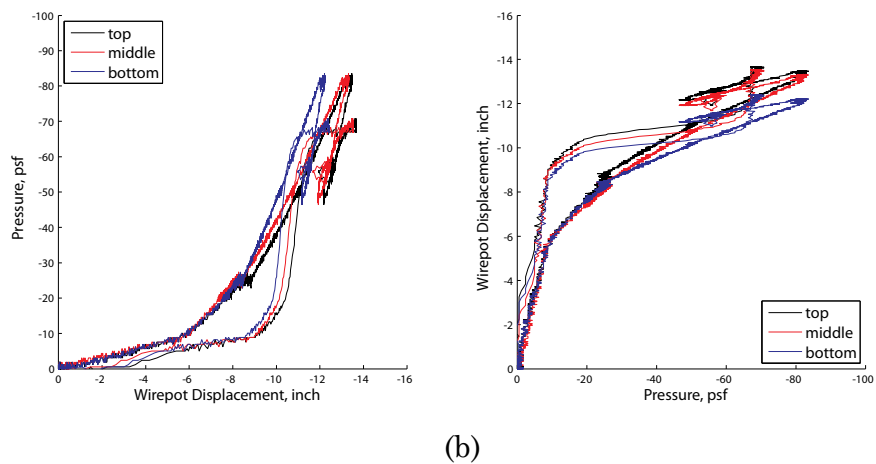
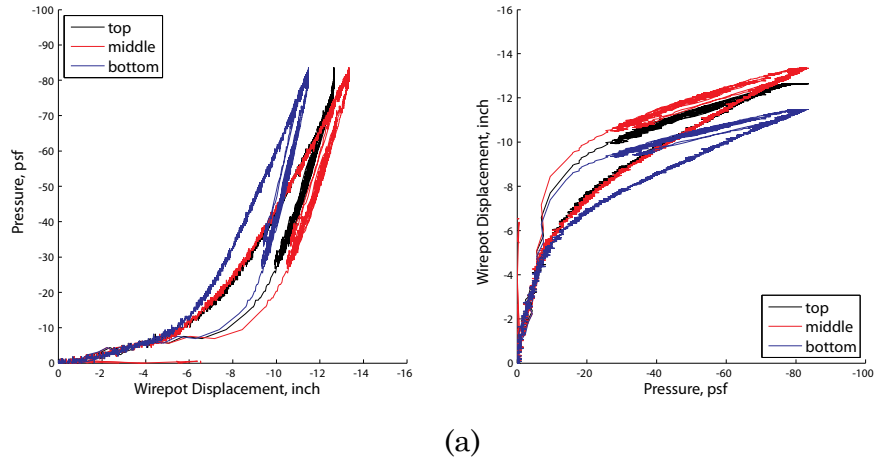
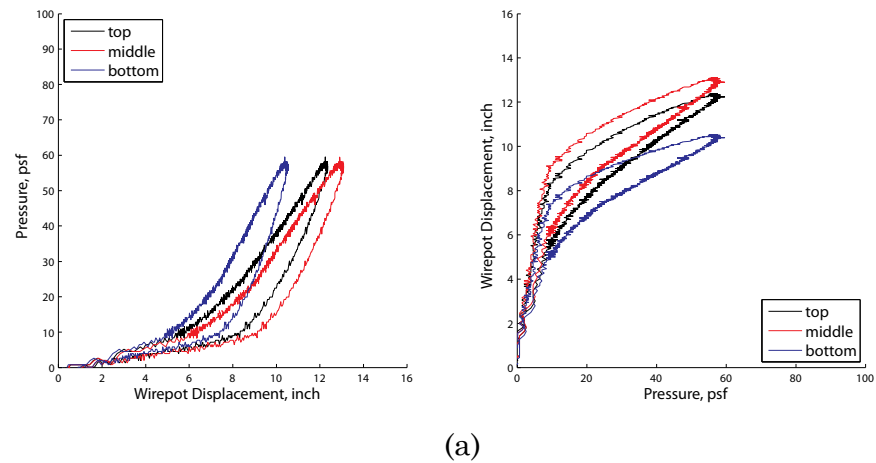
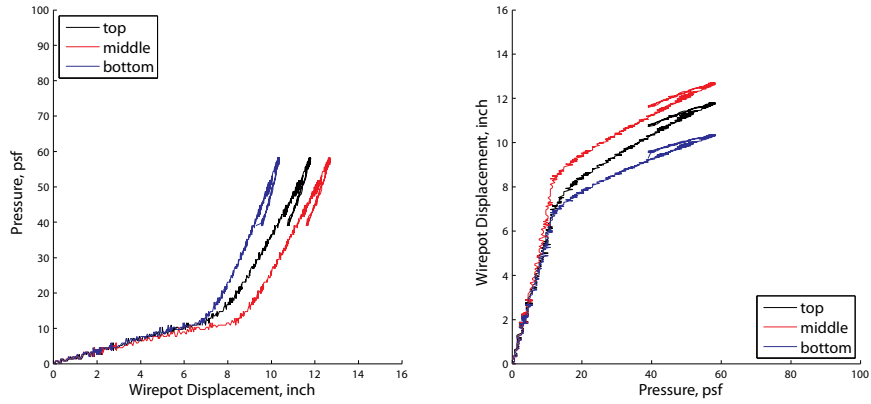


Figure 16. Curtain deflection in negative pressure for (a) Door#1N and (b) Door#2N





(b)

Figure 17. Curtain deflection in positive pressure for (a) Door#1P-1 and (b) Door#1P-2

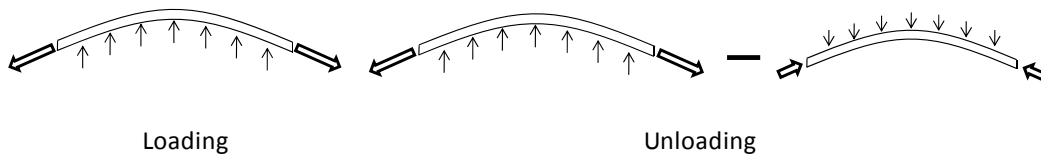


Figure 18. Arching action results in a higher unloading stiffness

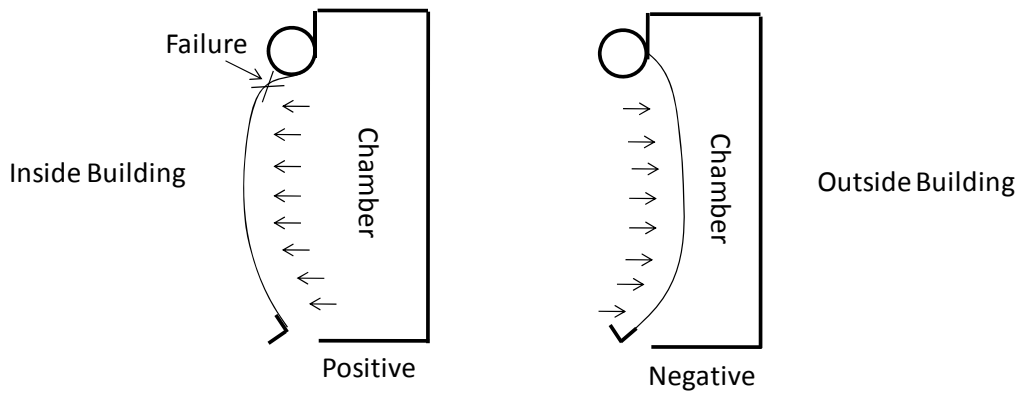


Figure 19. Curtain deflected shape varies with a positive or negative pressure



Figure 20. Bottom door angle was severely deformed after Door #1P-3 (+140 psf max)

The influence of multiple positive pressure loading sequences on a door is demonstrated in Figure 22. In the first positive pressure test on Door #1, Door #1P-1, the wind locks engaged the wind bar at approximately +6 in. of middle wire pot deflection. In the second positive pressure test on Door #1, Door #1P-2, the wind locks did not engage the wind bar until the middle wire plot deflected approximately +8 inch. Note that Door #1P-2 was tested shortly after Door #1P-1 without replacing the door frame or jambs. The 2 in. difference is hypothesized to occur because of a permanent in-plane displacement of the jamb after the Door #1P-1 testing. This could have occurred due to permanent deformation in the jamb or slippage in the bolted connection of the girt to the jamb, permanent deformation in the wind lock, or binding of the sheet door in the guide. (Note that oversized holes were used in the bolted connections.) The results are consistent with preliminary finite element model results, where a small in-plane displacement in the jamb of 0.10 in. resulted in an out-of-plane deflection of the curtain of approximately 2 in. Furthermore, the Door #1P-2 test has a higher loading stiffness (steeper slope in Figure 22) than Door #1P-1 test, supporting the hypothesis that the jamb stiffness increased in the second from full bearing in the bolted connections.

The difference in pressure-deformation response of the door between a positive pressure test and negative pressure test can be observed in Figure 23. Door #1N has a higher loading stiffness than Door #1P-1. It is hypothesized that the higher stiffness in the negative pressure tests occurs, at least in part, because of the direction of the catenary forces on the jamb. As shown in Figure 24, the jamb is inherently stiffer in the direction of the catenary forces applied by the negative pressure test when compared to those applied by a positive pressure test because the moment arm between the catenary force and the pivot point on the jamb is smaller in the negative pressure test as shown in Figure 24.

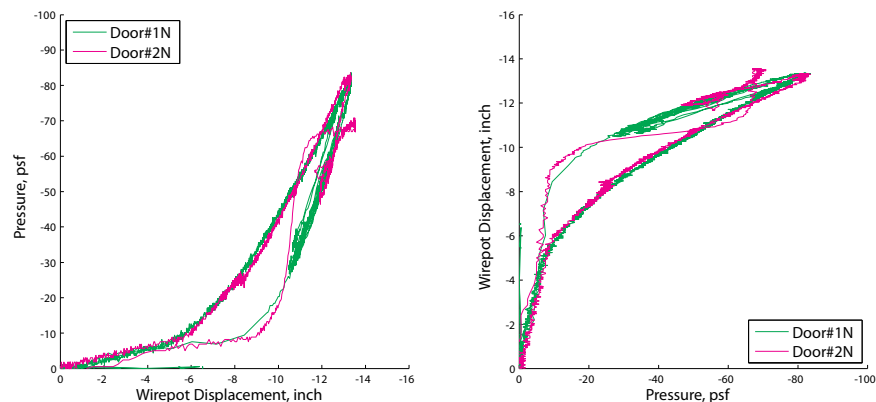


Figure 21. Deflection of the middle in the curtain in negative pressure

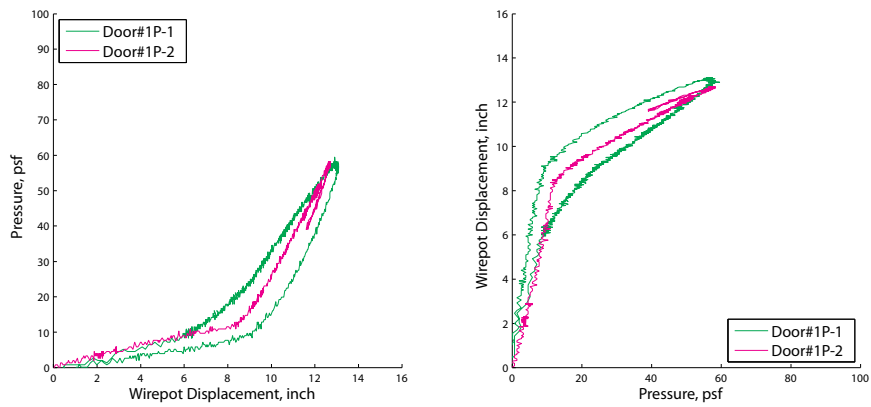


Figure 22. Deflection of middle curtain in positive pressure

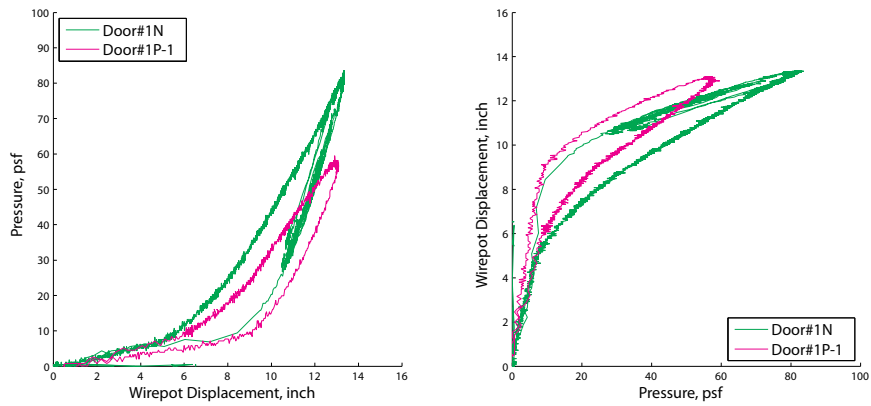


Figure 23. Deflection of middle curtain in negative and positive pressure

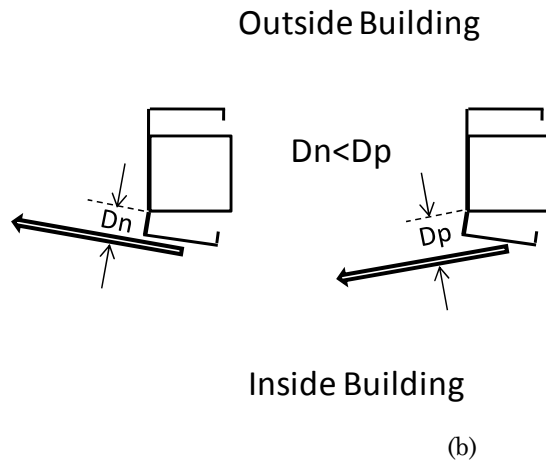


Figure 24 Direction of catenary forces on the jamb in (a) the negative pressure test and (b) the positive pressure test

2.4.2 Axial Force in Wind Lock vs. Pressure

The axial force, P , per wind lock, as calculated from the strains in the negative and positive pressure testing in Eq. (1), are summarized in Figure 25 and Figure 26. (Strain A and Strain B in each wind lock for each test is provided in Appendix E). For the negative pressure tests in Figure 25, the axial force does not develop until the wind lock engages the wind bar between -10 psf and -30 psf. (This trend is consistent with the pressure-displacement curves in Figure 16.) After wind lock engagement, the axial force increases as pressure is applied, confirming that catenary forces are influenced by the interaction between the curtain and the jamb. The axial force at -80 psf (Door #1N) ranges between -200 lbs compression to +650 lbs tension as summarized in Figure 27 and Table 1. The maximum measured wind lock force is approximately 50% lower than that predicted force of 1220 lbs per wind lock corresponding to a negative pressure of 80 psf interpolated from the DASMA sample calculations summarized in Appendix D.

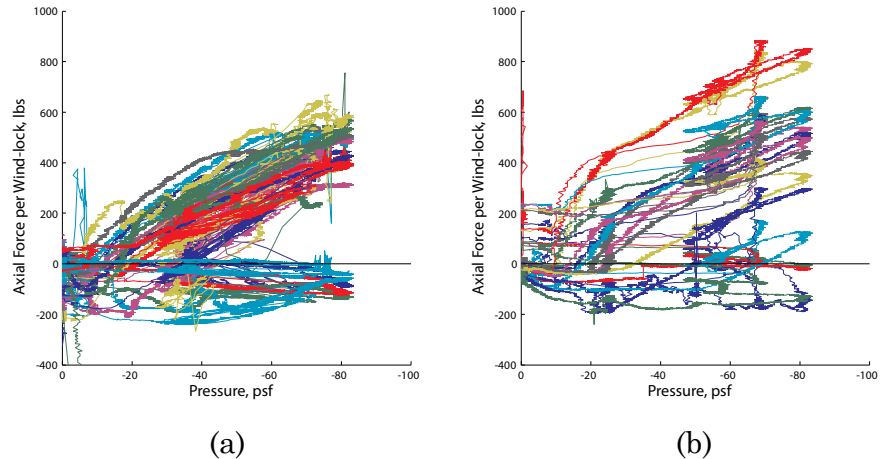


Figure 25. Axial forces per wind lock for (a) Door #1N and (b) Door #2N. Data for wind lock #5 and #17 in Door #2N were removed because of failed strain gauges. See Appendix E.

The wind lock axial forces for the positive pressure tests are provided in Figure 26, and demonstrate a similar trend to the negative pressure tests. The axial force increases after 10 psf and the wind locks engage. At +80 psf (Door #1P-1), the axial force at each wind lock ranged from -75 lbs to +450 lbs as summarized in Figure 27 and Table 1. There is no observable correlation between girt location and wind lock forces (Figure 26).

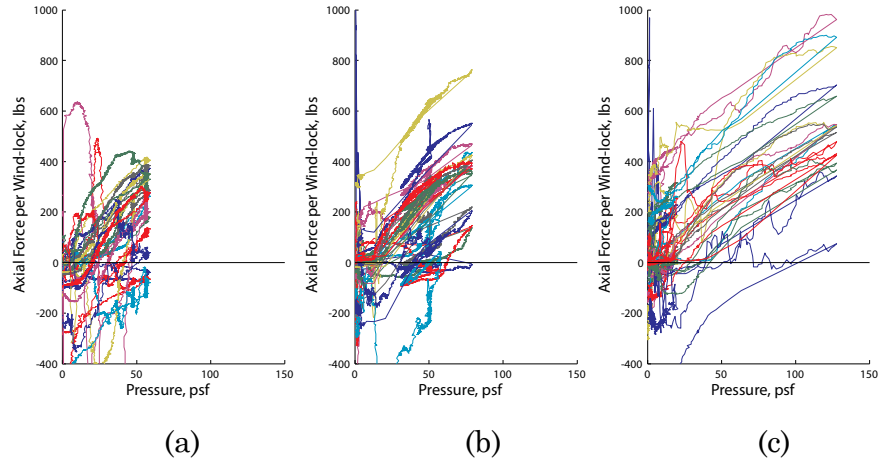


Figure 26. Axial forces per wind locks. (a) Door #1P-1, (b) Door #1P-2 and (c) Door #1P-3. Data for wind lock #1 in all positive pressure tests was removed due to a failed strain gauge (see Appendix E)

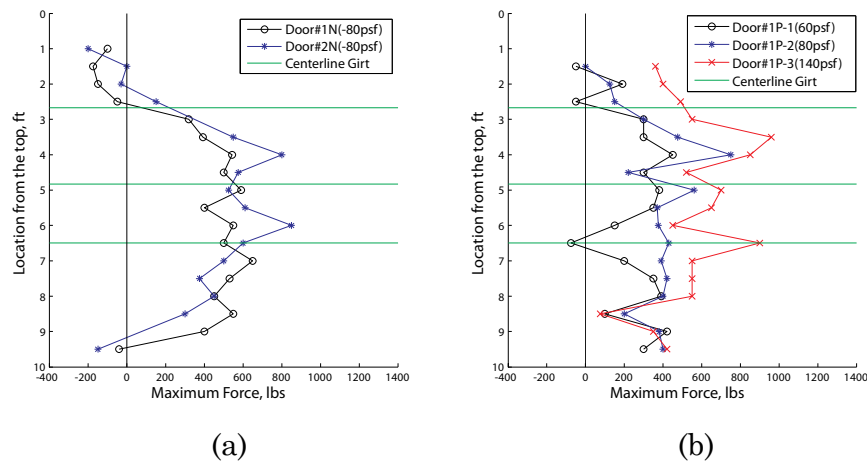


Figure 27. Maximum axial forces per wind lock for (a) negative pressure and (b) positive pressure tests. Data for wind lock #5 and #17 in Door #2N, and data for wind lock #1 in all positive pressure tests were removed because of a failed strain gauge. See Appendix E.

Table 1 Summary of maximum wind lock axial forces

Location from top of door	Door #1N (-80 psf)	Door #2N (-80 psf)	Door #1P1 (+60 psf)	Door #1P2 (+80 psf)	Door #1P3 (+140 psf)
ft.	lbs	lbs	lbs	lbs	lbs
1	-100	-200			
1.5	-175	0	-50	0	360
2	-150	-30	190	125	400
2.5	-50	150	-50	150	490
3	320		300	300	550
3.5	390	550	300	475	960
4	540	800	450	750	850
4.5	500	575	300	220	520
5	590	525	380	560	700
5.5	400	610	350	370	650
6	550	850	150	375	450
6.5	500	600	-75	430	900
7	650	500	200	390	550
7.5	530	375	350	420	550
8	450	450	390	400	550
8.5	550	300	100	200	75
9	400		420	380	350
9.5	-40	-150	300	400	420
Max	650	850	450	750	960
Min	-175	-200	-75	0	75

2.4.3 Bending Moment vs. Pressure

The moment in the wind locks at the gauge locations for both negative and positive pressure tests are shown in Figure 28 and Figure 29. In the negative pressure test (Figure 28), below -10 psf the wind locks are not engaged and the moments in the wind locks are negligible. After the wind locks engage, a positive moment increases as a function of pressure until reaching a constant magnitude at approximately -40 psf. The peak moments in each wind lock are summarized in Figure 30. The sign of the moment (i.e. a positive moment) is consistent with the observed deformation pattern for a negative pressure test as shown in Figure 31a. Figure 29 does not show any measurable effect of the girt location on the maximum moment.

For the positive pressure tests in Figure 29, the moment is initially negative, but then transitions to a positive moment at approximately +30 psf. This transition from negative to positive moment occurs as the wind lock contacts the wind guide as shown in Figure 31b, resulting in double curvature in the wind lock and a reversal of moment (Figure 32), and ultimately severe plastic deformation of the wind guide and wind bar (Figure 33). The moment plateaus and slightly decreases for all positive

pressure tests (Figure 29) due to yielding of the wind lock and/or the wind guide.

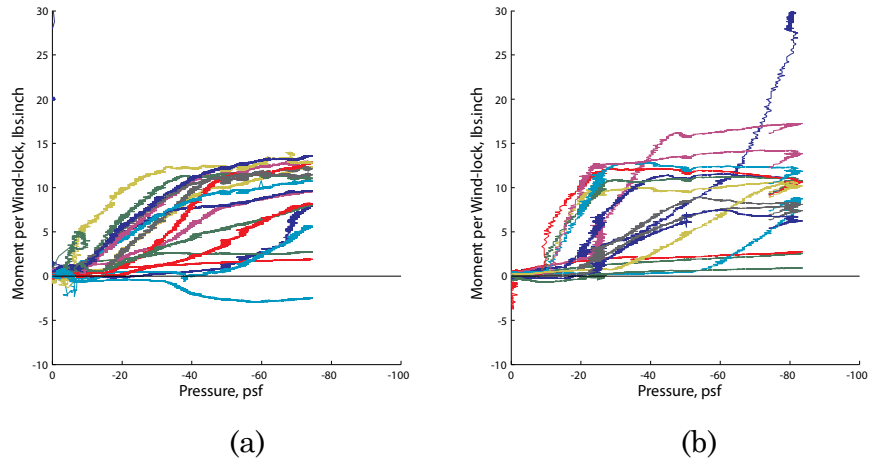


Figure 28. Moment at gauge location per wind lock in negative pressure. (a) Door #1N and (b) Door #2N. To clarify the figure, the unloading portion of the curve was removed. Data for wind lock #5 and #17 in Door #2N were removed because of failed strain gauge. See Appendix E.

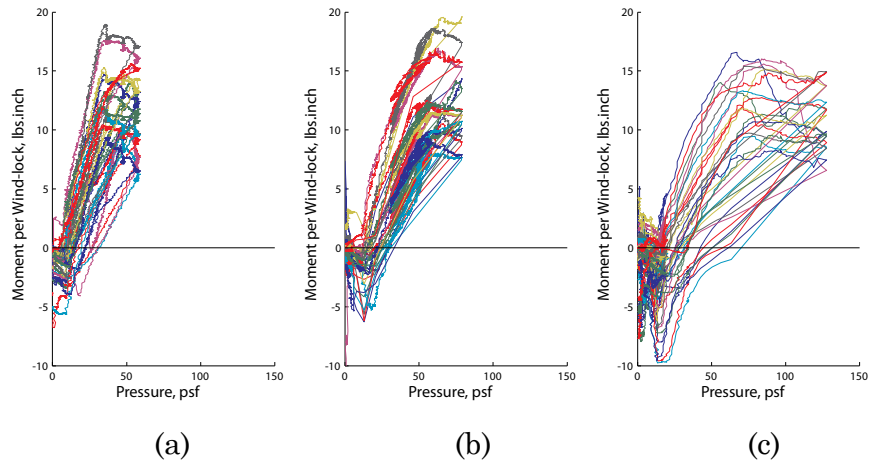


Figure 29. Moment at gauge location per wind lock in positive pressure. (a) Door #1P-1, (b) Door #1P-2 and (c) Door #1P-3. Data for wind lock #1 in all positive pressure testing was removed due to failed strain gauge. See Appendix E

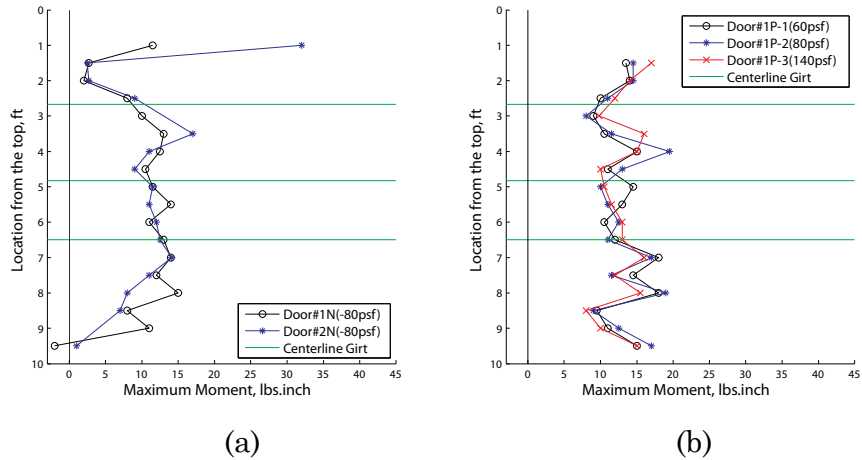


Figure 30. Maximum bending moment at gauge location per wind lock for (a) negative and (b) positive pressures. Data for wind lock #5 and #17 in Door #2N, and data for wind lock #1 in all positive pressure tests were removed because of a failed strain gauge. See Appendix E.

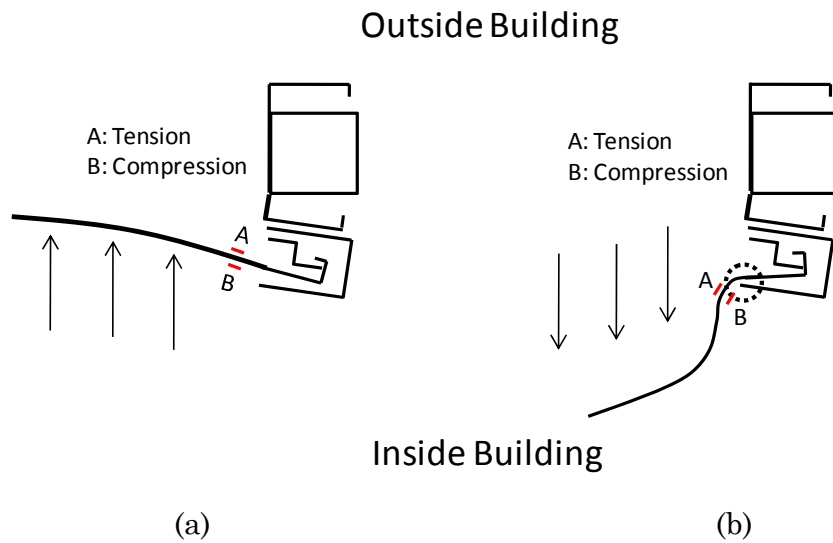


Figure 31. Wind lock system in (a) negative and (b) positive pressure

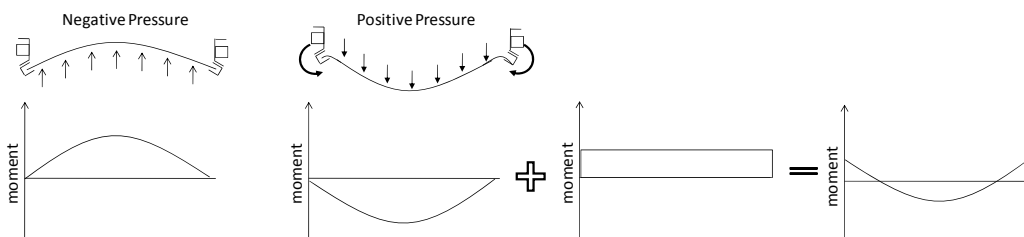


Figure 32: Moment diagram in negative and positive pressure



Figure 33. Bended wind lock and wind-guide after positive testing

2.5 Jamb Displacement vs. Pressure

The in-plane displacement of the jamb, a , was measured with LVDT-1 (see Figure 14). By observing the slope of the pressure-displacement curves in Figure 34, the jamb behavior in the negative pressure testing is concluded to be stiffer than in positive pressure testing, supporting the hypothesis proposed in Section 2.4.1 and described in Figure 24. Note that the in-plane displacement measurement with LVDT-1 is a combination of jamb flange-web rotation (Figure 14a) and global deformation of the door frame which could not be separated with the measurements taken during the experiments. Also note that the out-of-plane jamb measurements from LVDT-2 (see Figure 14b) were deemed unreliable and are not presented here.

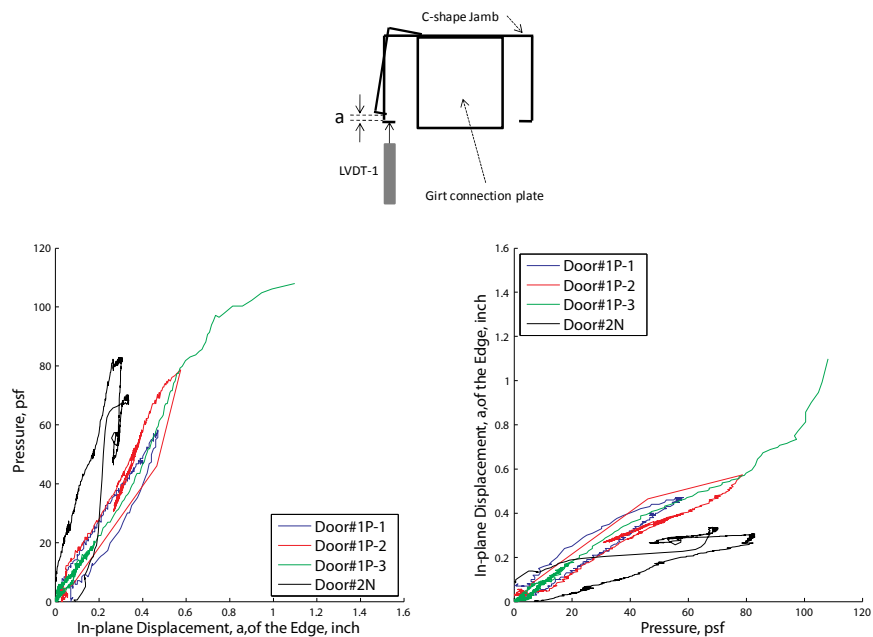


Figure 34. In-plane displacement of the jamb due to the rotation of the flange



Figure 35. The web was plastically deformed at a seam corresponding to the welded girt connection plate

3 Conclusions

Wind pressure experiments were conducted on two steel curtain rolling sheet doors to quantify the catenary forces present in the wind locks and to evaluate overall structural behavior under both negative and positive pressure loadings. The out-of-plane door deformation increased rapidly until the wind locks engaged with the wind bar at ± 10 psf for both negative and positive pressure tests. Once the wind locks were engaged, the system stiffness increased, resulting in catenary forces that were an average less than 50% of the DASMA predictions for both positive and negative pressure on the building. The direction of the wind lock forces on the jamb was observed to influence the in-plane system stiffness, and there was no observed connection between girt location and wind lock force. For positive pressure on the building, the wind locks contacted the wind guide, causing plastic bending of the wind lock and the wind guide at pressures above +40 psf. The jamb flexibility was observed to be an important parameter when predicting the wind lock forces and the out-of-plane deflections of the rolling sheet door.

4 Future Work

Additional research is summarized in the following section which could improve wind lock force predictions and rolling sheet door design methods and details.

4.1 Jamb Flexibility

The flexibility of the door jamb has a significant effect on the performance of the door. A stiff jamb results in small deflections of the curtain but large catenary forces; a flexible jamb reduces the catenary forces but increases the deflection of the curtain. The present study only tells us that the flexibility of the jamb is caused by the rotation of the flange and the bending of the web as shown in Figure 36. Research is needed to quantify this flexibility (e.g., the stiffness associated with deformation of the jamb section ABC in Figure 36) with experiments and with analytical studies so that it can be incorporated into a rolling sheet door design.

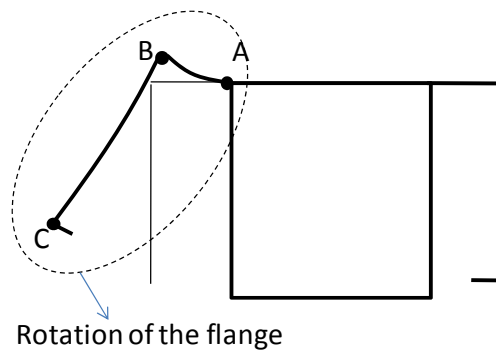


Figure 36. Rotation of the jamb flange plays a key role in the structural behavior of a rolling sheet door

Alternative jamb details should also be considered to improve the performance of the door. Jamb stiffness can be increased by orienting the open face of the C-section toward the door and making a closed section with an additional C-section screw-fastened at the flanges. The bolted girt connection detail could also be tailored to limit the flexibility of the jamb.

4.2 Finite Element Analysis

Preliminary static shell finite element (FE) analyses shown in Figure 37 initially identified the sensitivity of rolling sheet door performance and design loads to door frame stiffness. With the experimental data collected

in this study, a formal FE modeling protocol could be developed and validated, leading to a powerful tool for conducting parameter studies and deriving design charts and tables for steel curtain rolling sheet doors.

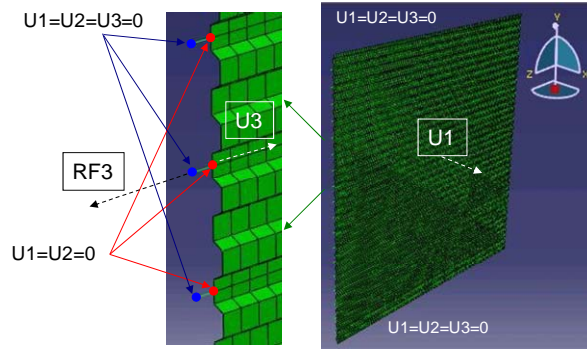


Figure 37 Preliminary FE model of a steel curtain rolling sheet door

4.3 Simplified Mechanics-Based Prediction Models

The experimental work and preliminary FE analyses have revealed the fundamental behavior of the structural system. This basic understanding can now be extended to mechanics-based models (Figure 38), leading to more general prediction equations for out-of-plane door deflection and wind lock forces. The equations derived from the model could be integrated into code-based language and design guides for rolling sheet door manufacturers and practicing engineers.

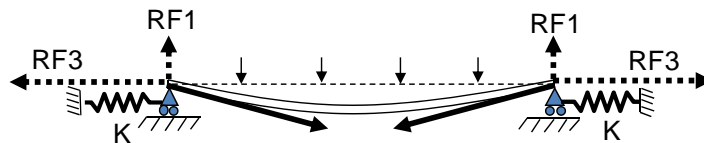


Figure 38. Proposed mechanics-based model describing the behavior of a rolling sheet door

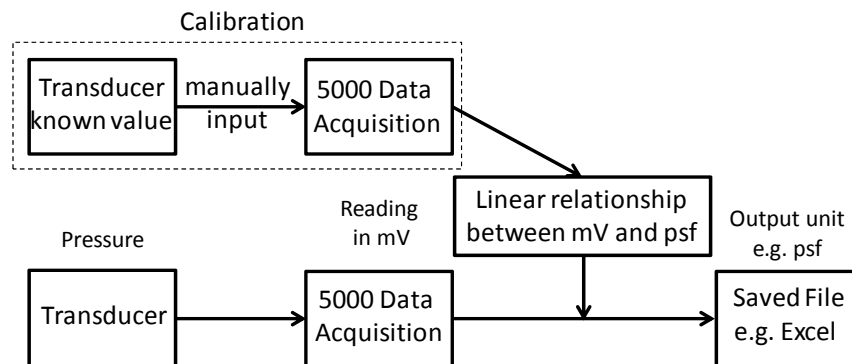
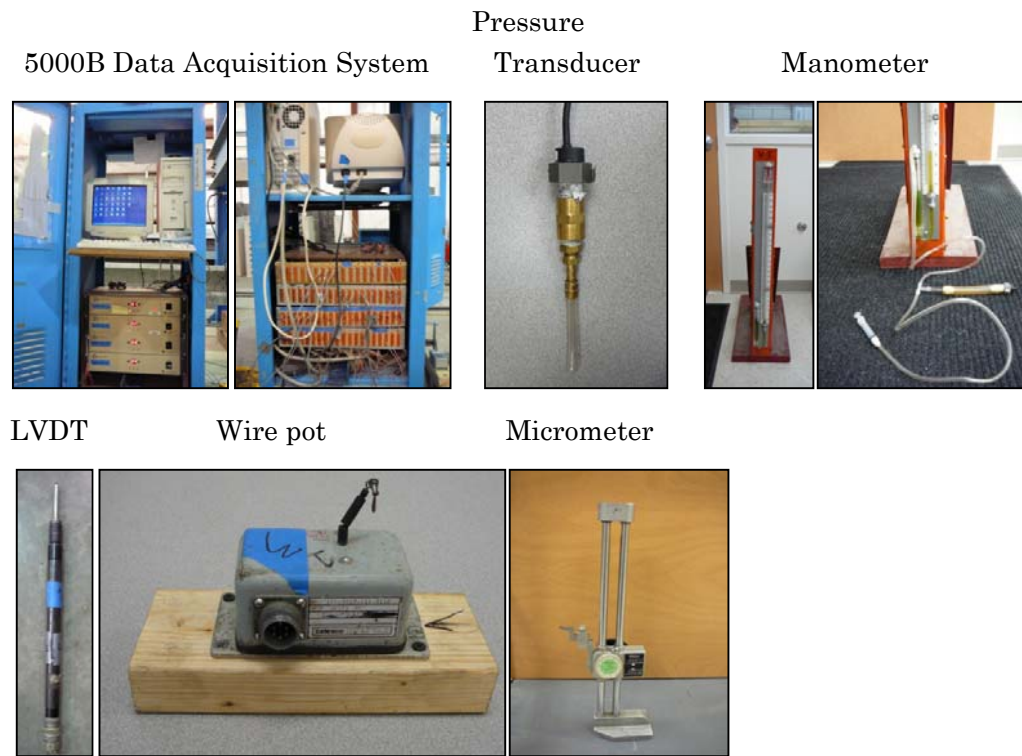
4.4 Experimental Testing

The interaction of the wind lock, wind bar, and wind guide is difficult to study because the connection is hidden from view. More full scale and component level testing (i.e. performing isolated tests of the wind bar and door jamb) are needed to observe and fully quantify the behavior of the structural system across the range of door systems and jamb types commonly employed in industry. Modified wind guide details or embedded video cameras could be used observe the behavior of the wind lock as pressure increases.

References

Ugural, A.C., and Fenster, S.K. (2003). *Advanced Strength and Applied Elasticity, Fourth Edition*, Prentice Hall, Upper Saddle River, NJ.

Appendix A – Gauge Calibration Procedures



The transducers were connected with 5000B Data Acquisition System. The measurement (pressure) in the transducer is input into the Data Acquisition System. The reading in the Data Acquisition System (mV) is converted into a set of units we prefer (psf) using a linear relationship between the (mV) value and (psf) value, and output into Microsoft Excel.

In the case of pressure transducer calibration, a manometer, syringe and a pressure transducer were connected in series. Eight pressures (± 1 , ± 2 , ± 3 and ± 4 inwc in manometer) were obtained by pushing or pulling on the

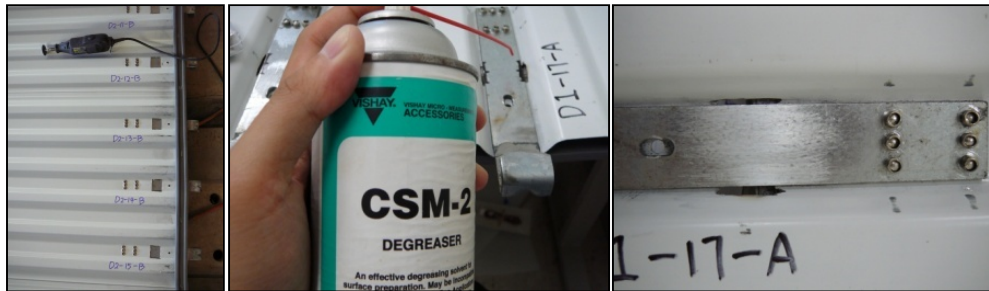
syringe. The reading in the manometer (inwc) was converted into (psf) by multiplying 5.2 and manually input into the Data Acquisition System to serve as the conversion between mV and incw.

Linear Variable Differential Transformer (LVDT) displacement transducer and wire potentiometers (wire pot) were calibrated in with a micrometer. Eight points for LVDT calibration were taken at ± 0.25 , ± 0.5 , ± 0.75 , and ± 1 inch, while eight points for wire pot calibration were at ± 1 , ± 2 , ± 3 , and ± 4 inch.

Appendix B - Strain Gauge Installation



- Strain gauges (C2A-13-250LW-350) were purchased from Vishay



- Small holes were sawn in the curtain so that the gauges can be installed in both sides of the wind lock. The wind lock was cleaned with degreaser, sanded with 200 grit sand paper and cleaned with neutralizer.

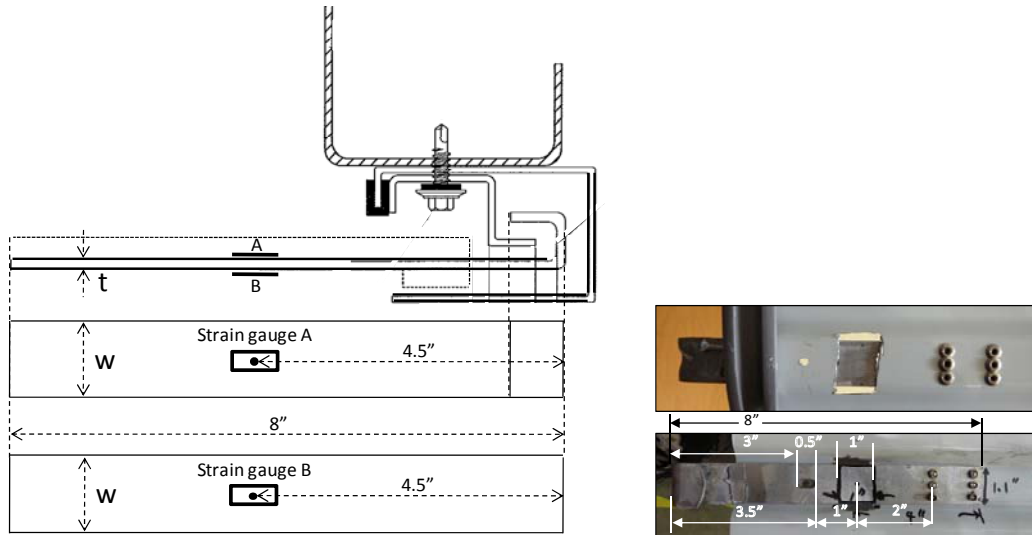


- The gauges were bonded with M-bond 200 adhesive and coated with air-curing polyurethane.



- The gauges were protected with a rubber layer and tape.

Appendix C - Wind Lock Dimensions



Wind-lock#	Door#1		Door#2	
	t (in.)	w (in.)	t (in.)	w (in.)
1	0.13	1.144	0.13	1.100
2	0.13	1.144	0.13	1.140
3	0.13	1.100	0.13	1.144
4	0.13	1.100	0.13	1.100
5	0.13	1.136	0.13	1.148
6	0.13	1.140	0.13	1.144
7	0.13	1.100	0.13	1.100
8	0.13	1.144	0.13	1.144
9	0.13	1.100	0.13	1.140
10	0.13	1.100	0.13	1.100
11	0.13	1.100	0.13	1.100
12	0.13	1.100	0.13	1.144
13	0.13	1.100	0.13	1.100
14	0.13	1.100	0.13	1.136
15	0.13	1.132	0.13	1.144
16	0.13	1.100	0.13	1.100
17	0.13	1.156	0.13	1.100
18	0.13	1.142	0.13	1.144

Appendix D – DASMA Rolling Sheet Door Calculations

Applied Forces and Moments

DBCI Door Series 5000 - used in 8/09 MBMA Research

Test

Calculations by Joseph H. Dixon, Jr., 8/19/09

Given:

WL = Wind Load = +/-60.0 PSF

L = Door Width = 10.5 Ft.

P = Slat Pitch = 3.21 In.

I = Slat Moment of Inertia = .00425 In⁴ (per slat)

It= Total Moment of Inertia = 12/P x I = . 01589 In⁴ (per ft. door ht.)

E = Slat Modulus Elasticity = 30,000,000 P.S.I.

WS = Windlock slip or Windlock Gap = .3125 In.

SO= Guide standout or wall to wind bar dimension = 1.037 In.

OFS = Guide dimension wind bar to edge of opening = 1.6875 In.

Determine The Following:

1. **D** = Slat deflection before windlocks engage. (Ft.)
2. **W1** = Bending load for slat deflection. (Lbs./ft²)
3. **W2** = Wind load resisted after windlocks engage. (Lbs./ft²)
4. **C** = Catenary force for windlock slat tension load. (Lbs./ft. of door ht.)
5. **TH** = Angle of windlock pull. (Deg.)
6. **FX** = Force on windbar inside the guide in the “X” direction. (Lbs./Ft. of door ht.)
7. **FY** = Force on windbar inside the guide in the “Y” direction. (Lbs./Ft. of door ht.)
8. **Pos M** = Positive moment at corner of door opening with +WL interior mount (in-lbs.)
9. **Neg M** = Negative moment at corner of door opening with -WL interior mount (in-lbs.)

1. Slat deflection before windlocks engage. (ft.) [based reference 4]

$$D = (L \times WS)^{1/2} / 4 = .453 \text{ ft.} = 5.433 \text{ in.}$$

2. Bending load for slat deflection. (Lbs./ft²) [based on reference 1]

$$W1 = (24 \times E \times I_t \times D) / (45 \times L^4) = 6.7 \text{ psf}$$

3. Wind load resisted after wind locks engage. (Lbs./ft²) [simple sum of wind load forces]

$$W2 = WL - W1 = 53.3 \text{ psf}$$

4. Forces on wind bar inside the guide in the "X" direction. (Lbs./Ft. of ht.) [based on reference 3]

$$FX = W2 \times L^2 / 8 \times D = 1621 \text{ lbs./ft of door height}$$

5. Forces on wind bar inside the guide in the "Y" direction. (Lbs./Ft. door of ht.) [sum forces in the y direction equal zero]

$$FY = WL \times L / 2 = 315 \text{ lbs./ft. of door height}$$

6. Catenary force for wind lock slat tension load. (Lbs./ ft of door ht.) [based on reference 3]

$$C = FX \times (1 + (16 \times (D / L)^2))^{1/2} = 1645 \text{ lbs./ft. of door height}$$

7. Angle of slat to guide. (Deg.) [resultant angle of two know forces]

$$TH = \text{Cos}^{-1} (FX / C) = 9.8 \text{ Degrees}$$

8. Wall Moments based on the guide standout value (In-lbs/ ft. of door ht.) [Sum moments about the corner of the opening. See guide drawing for location and direction]

$$\text{Pos M} = FX \times SO - FY \times OFS = 1150 \text{ in-lbs}$$

$$\text{Neg M} = FX \times SO + FY \times OFS = 2213 \text{ in-lbs}$$

Engineering References

1. Source of the equations for deflection and moment:

AISC Steel Construction Manual, Allowable Stress Design, Uniformly Loaded Beam Unrestrained at the ends

$$\text{Deflection} = 5WL^4/384EI$$

$$\text{Moment} = WL^2/8$$

2. Roark & Young Formulae for Stress & Strain, Beams: Flexure of Straight Bars,
for Moment = $WL^2/8$.

*3. Source of catenary tension equation:

Structural Engineering Handbook, Gaylord & Gaylord, 1989

$$T = (QL_w^2/8F) \times (1+16(F/L_w)^2)^{0.5}$$

T = Catenary tension, lbs

Q = load, lbs/in

L_w = distance between where windlocks engage, in

F = deflection @ center of slat, in

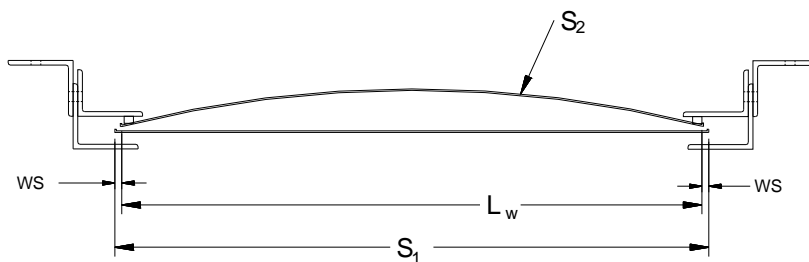
$$H = (QL_w^2/8F)$$

H = Horizontal Tension, lbs

*4) Source for Deflection Equation:

Based on Handbook of Engineering Mathematics, American Society of Metals (ASM) (Page 65 For Catenary)

$$D = (L_w \times WS)^{1/2} / 4, \text{ where } D = \text{Deflection (Ft.)}, L_w = \text{Door Width (Ft.)}, WS = \text{Windlock Slip (In.)}$$



Solve for "D"

$$S_1 = S_2$$

$$S_1 = L_w + 2WS/12$$

$$S_2 = L_w [1 + 2/3 (2D/L_w)^2]$$

$$L_w + (2WS/12) = L_w [1 + 2/3 (2D/L_w)^2]$$

$$2/3 \times 4D^2/L_w^2 = 8D^2/3L_w^2$$

$$L_w + (2WS/12) = L_w + L_w (8D^2/3L_w^2)$$

$$2WS/12 = L_w + 8D^2/3L_w - L_w$$

Subtract L_w from both sides and factor out L_w

$$WS/12 = (8D^2/3L_w) / 2$$

Divide by 2 each side = $8D^2/6L_w$

$$WS = (8D^2/6L_w) 12$$

Multiply by 12 each side = $96D^2/6L_w$

$$WS = 96D^2/6L_w = 16D^2/L_w$$

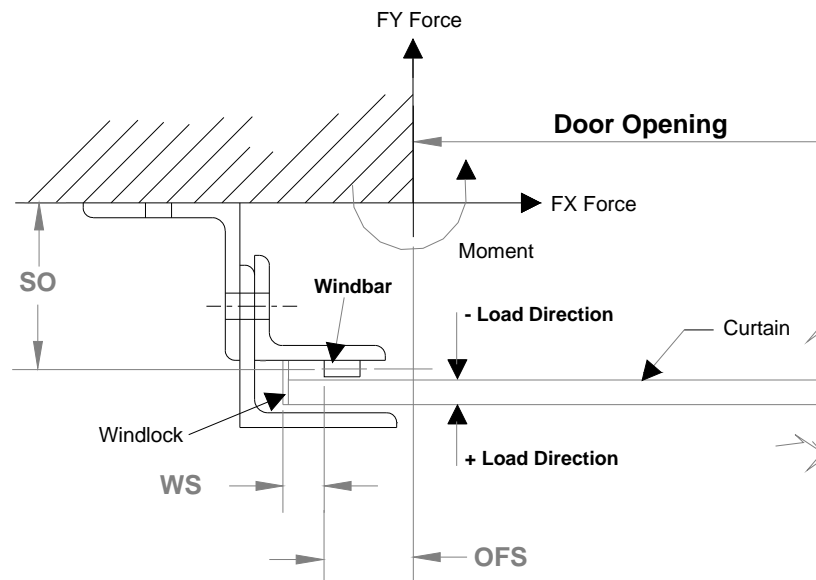
$$D^2 = (L_w WS) / 16$$

$$D = (L_w WS)^{1/2} / 4$$

Square root each side

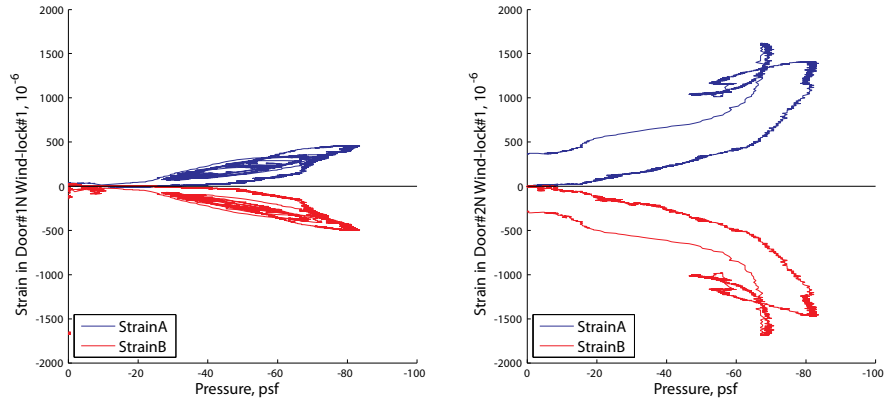
* For ease of calculations, door width is used in place of L_w

Drawing Illustrating Equation Variables

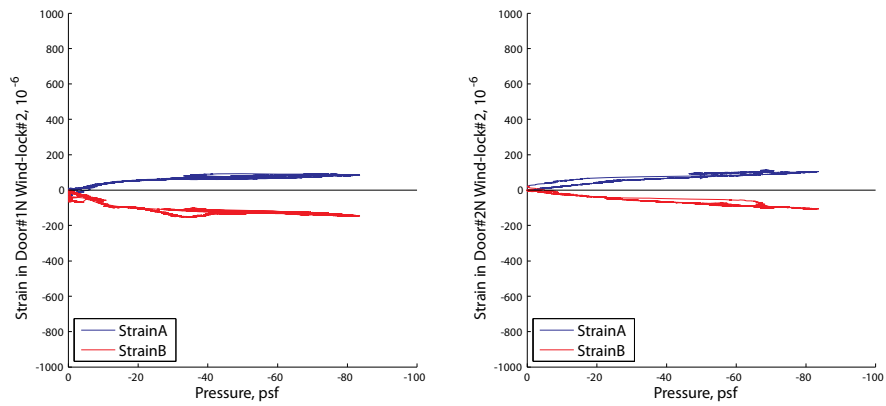


Appendix E - Wind Lock Strains

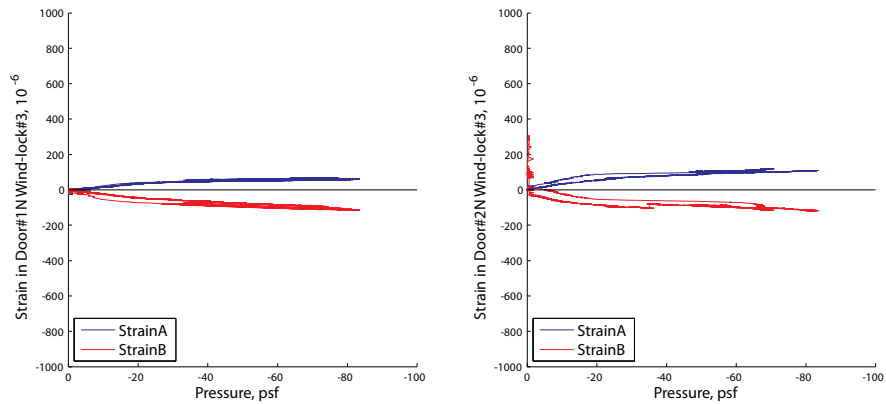
Negative Pressure Testing



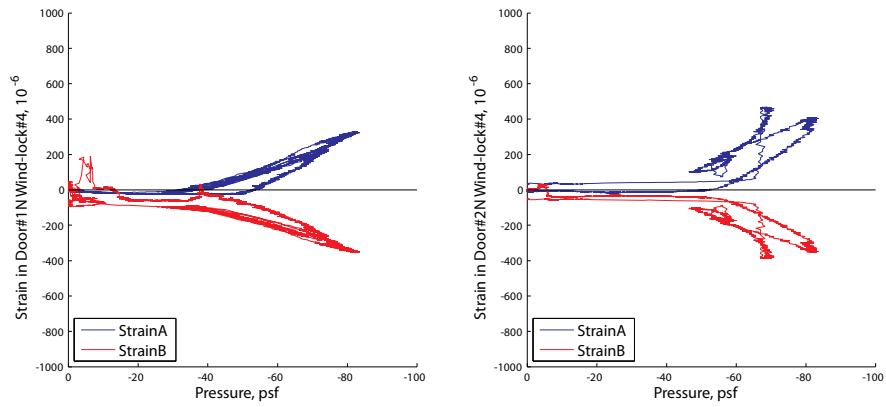
Strain in wind lock#1 in Door#1N (left) and Door#2N (right)



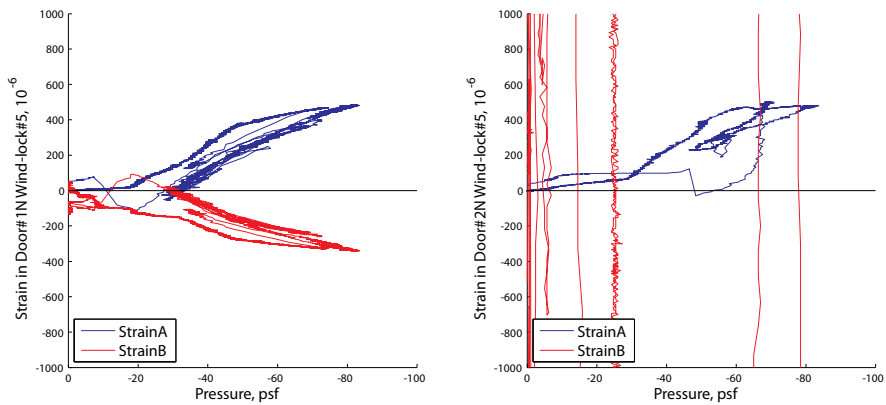
Strain in wind lock#2 in Door#1N (left) and Door#2N (right)



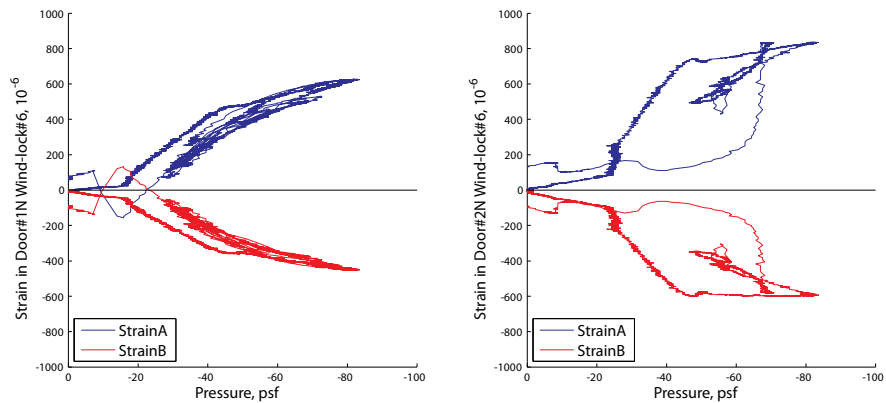
Strain in wind lock#3 in Door#1N (left) and Door#2N (right)



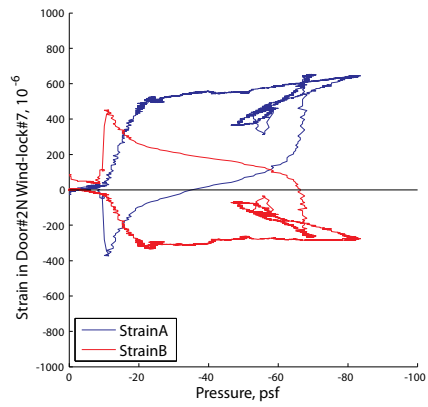
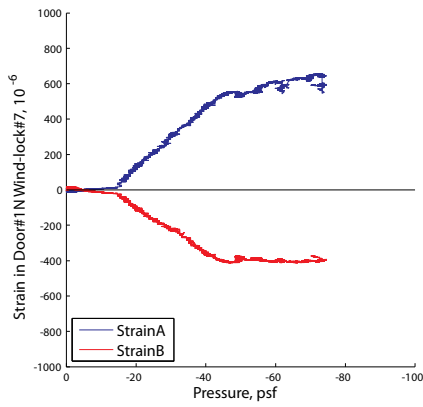
Strain in wind lock#4 in Door#1N (left) and Door#2N (right)



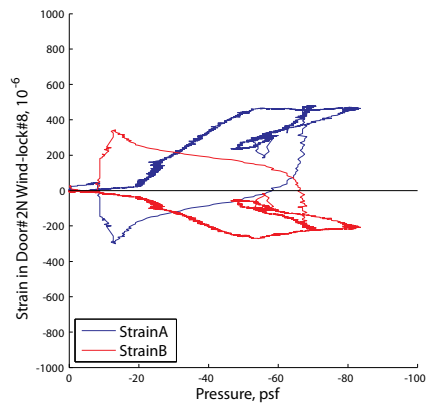
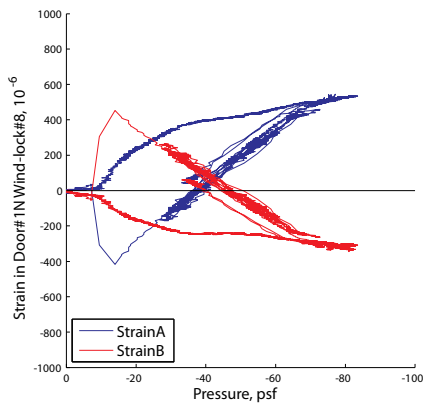
Strain in wind lock#5 in Door#1N (left) and Door#2N (right). GaugeB in Door#2 was failed and removed.



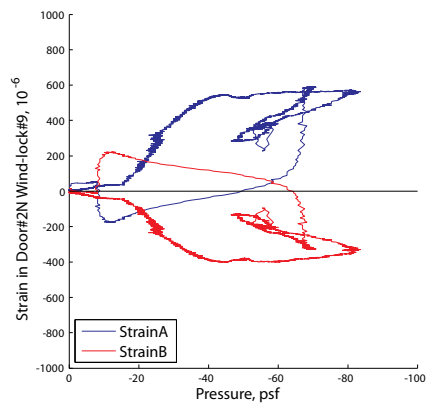
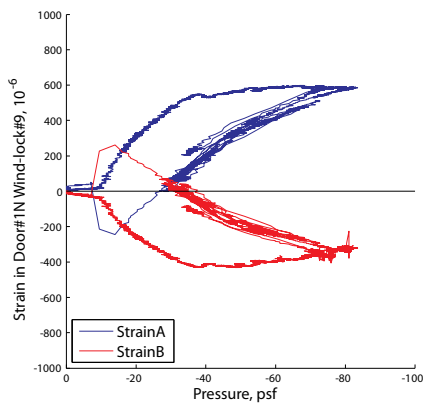
Strain in wind lock#6 in Door#1N (left) and Door#2N (right)



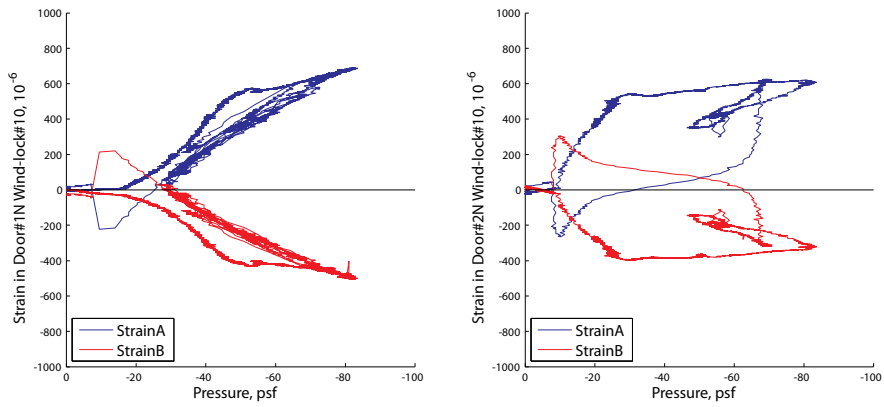
Strain in wind lock#7 in Door#1N (left) and Door#2N (right)



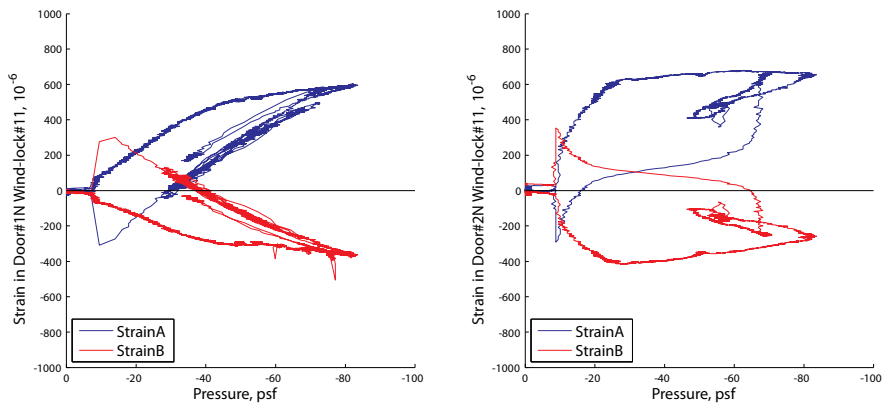
Strain in wind lock#8 in Door#1N (left) and Door#2N (right)



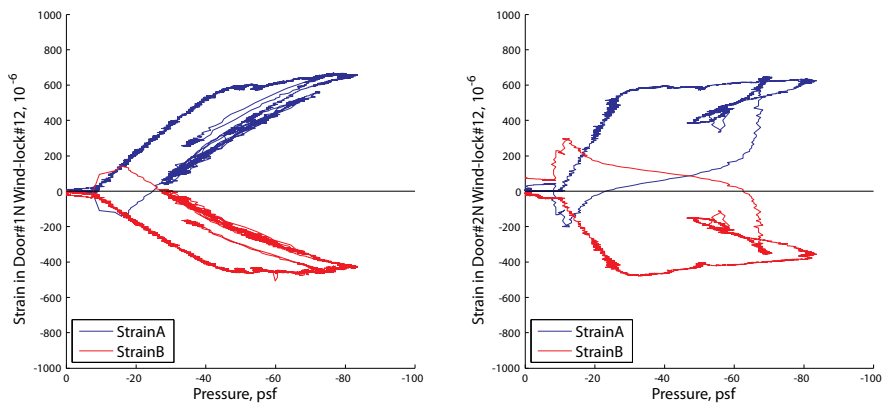
Strain in wind lock#9 in Door#1N (left) and Door#2N (right)



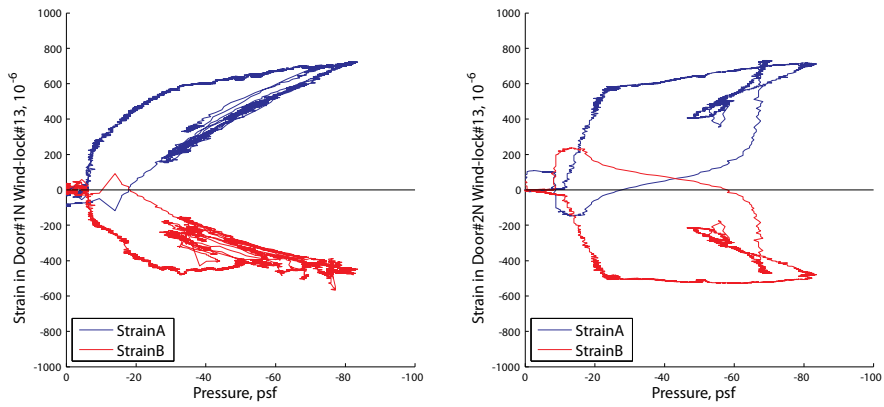
Strain in wind lock#10 in Door#1N (left) and Door#2N (right)



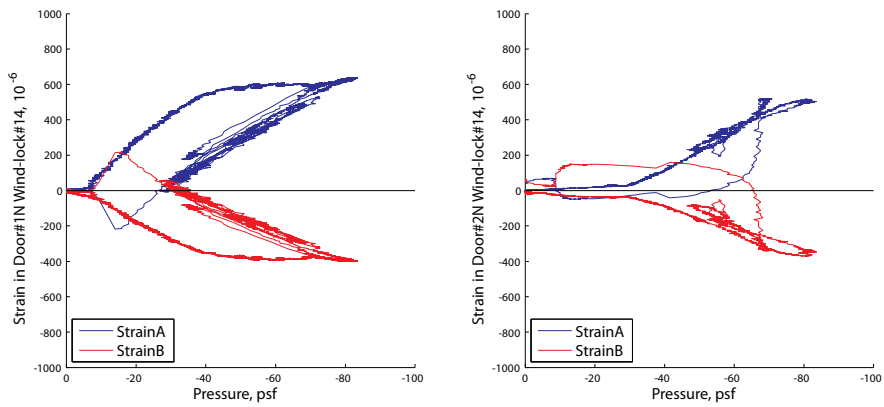
Strain in wind lock#11 in Door#1N (left) and Door#2N (right)



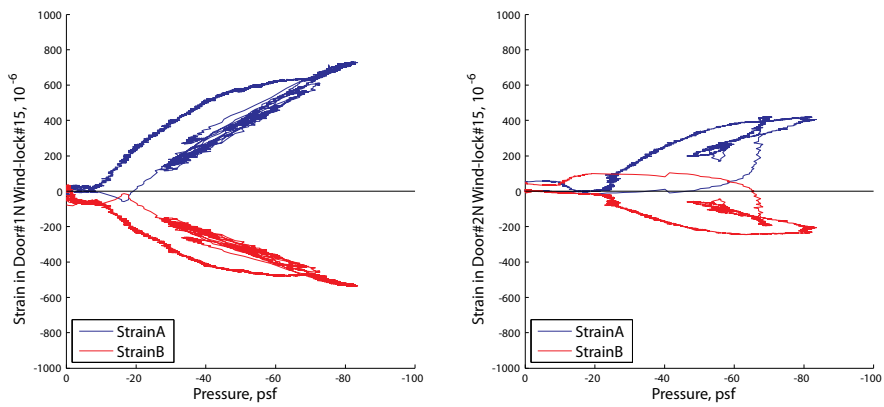
Strain in wind lock#12 in Door#1N (left) and Door#2N (right)



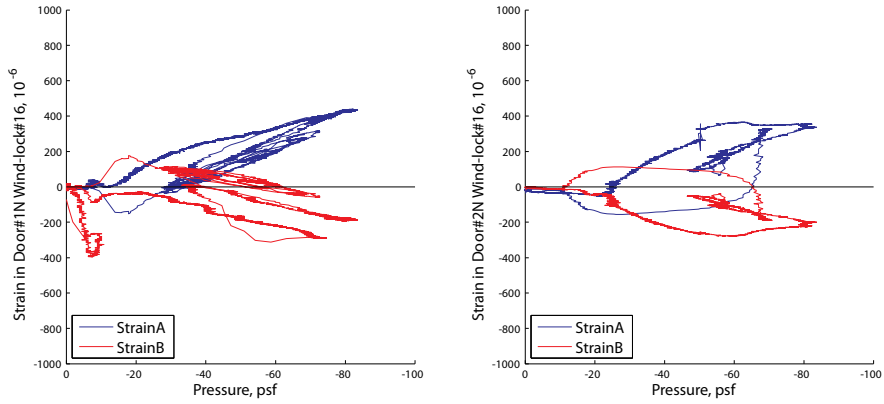
Strain in wind lock#13 in Door#1N (left) and Door#2N (right)



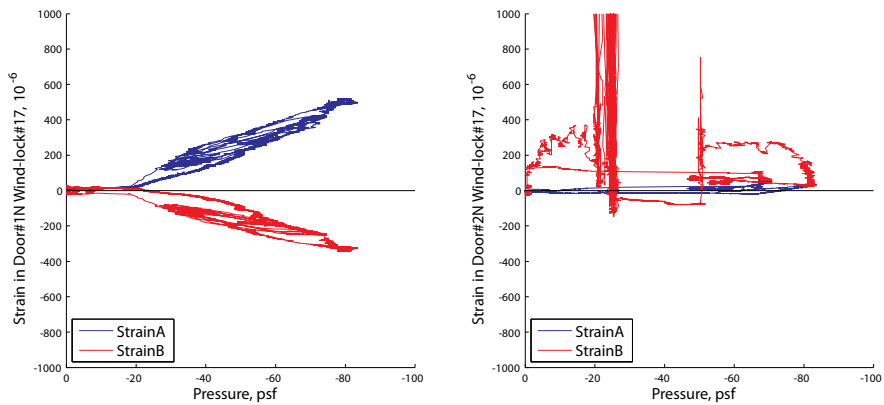
Strain in wind lock#14 in Door#1N (left) and Door#2N (right)



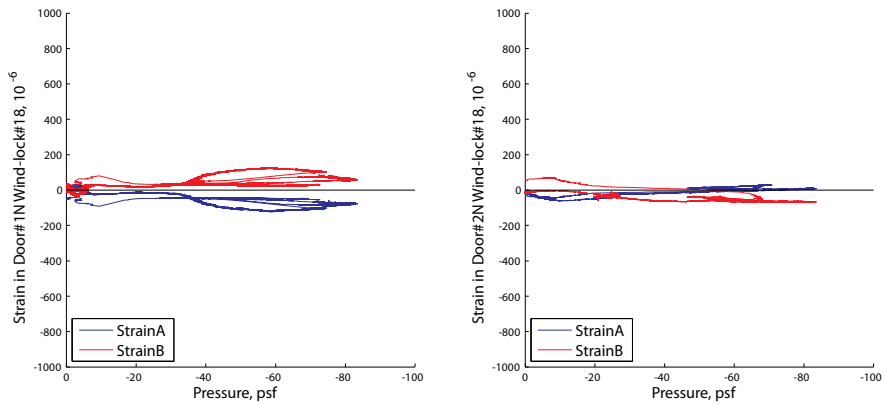
Strain in wind lock#15 in Door#1N (left) and Door#2N (right)



Strain in wind lock#16 in Door#1N (left) and Door#2N (right)

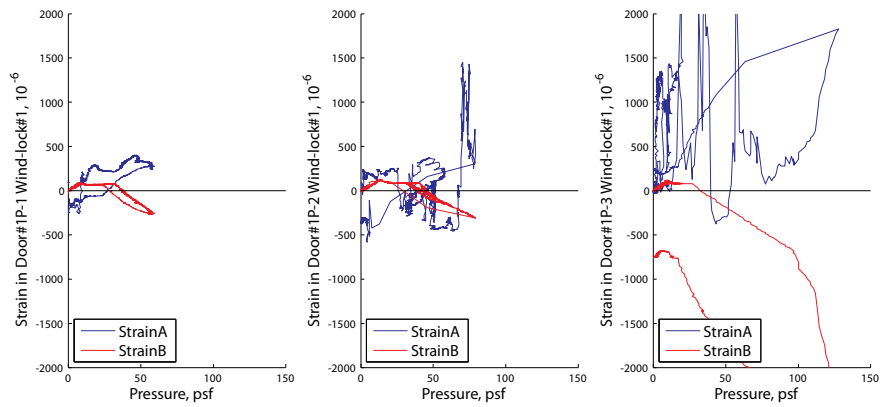


Strain in wind lock#17 in Door#1N (left) and Door#2N (right). GaugeB in Door#2 was failed and removed.

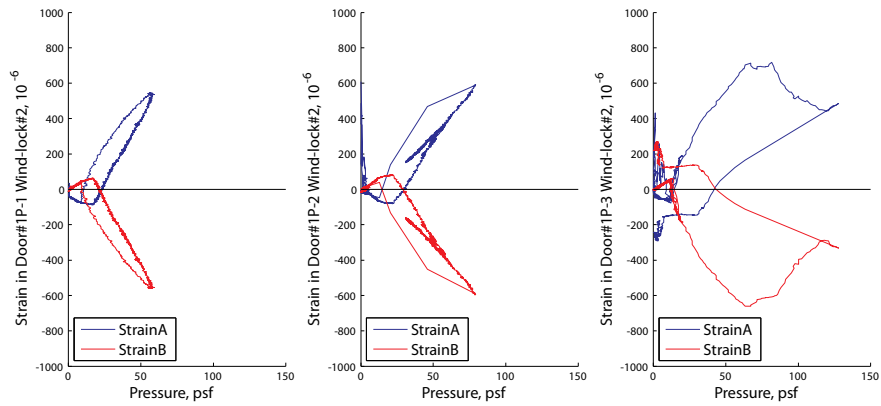


Strain in wind lock#18 in Door#1N (left) and Door#2N (right).

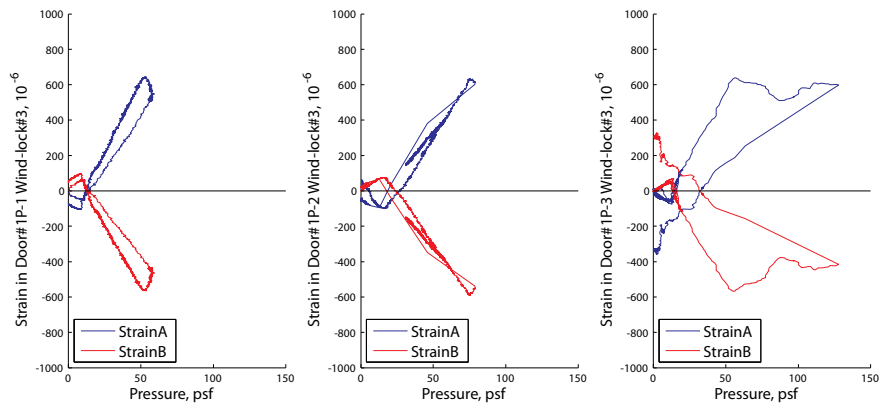
Positive Pressure Testing



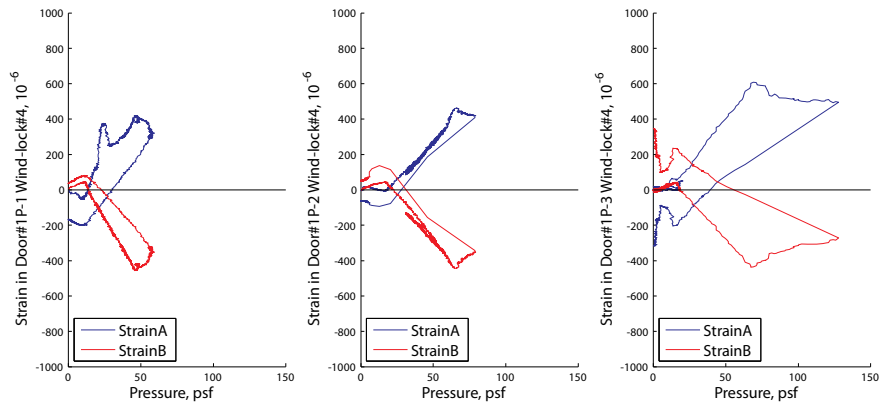
Strain in wind lock#1 in Door#1P-1 (left), Door#1P-2 (middle) and Door#1P-3(right). All data for wind lock#1 was removed.



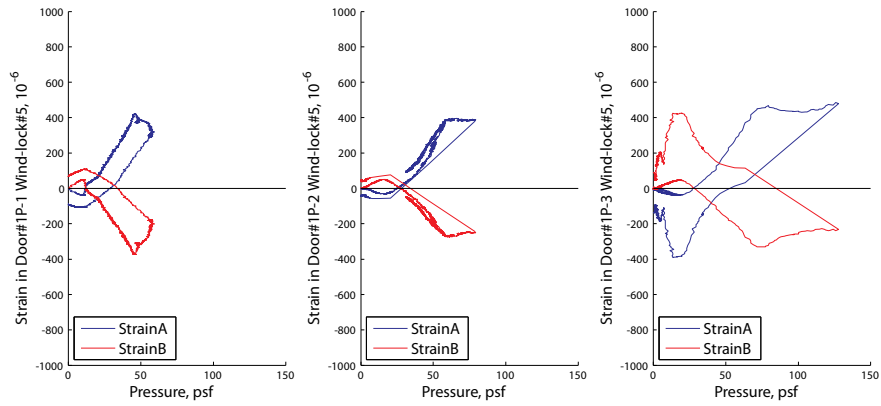
Strain in wind lock#2 in Door#1P-1 (left), Door#1P-2 (middle) and Door#1P-3(right)



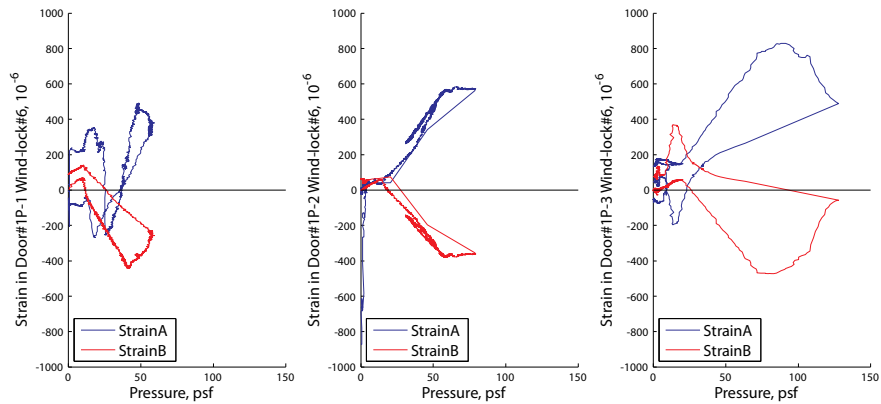
Strain in wind lock#3 in Door#1P-1 (left), Door#1P-2 (middle) and Door#1P-3(right)



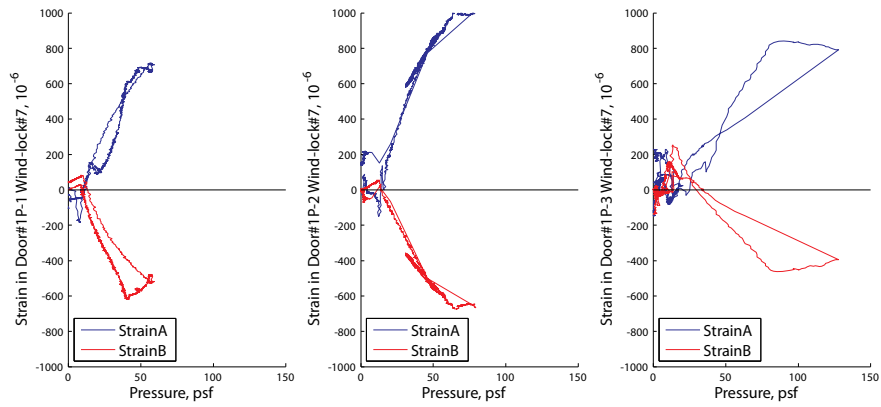
Strain in wind lock#4 in Door#1P-1 (left), Door#1P-2 (middle) and Door#1P-3(right)



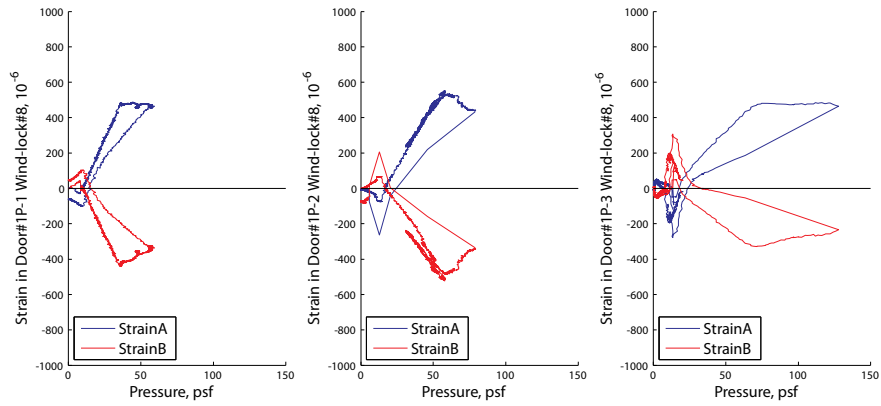
Strain in wind lock#5 in Door#1P-1 (left), Door#1P-2 (middle) and Door#1P-3(right)



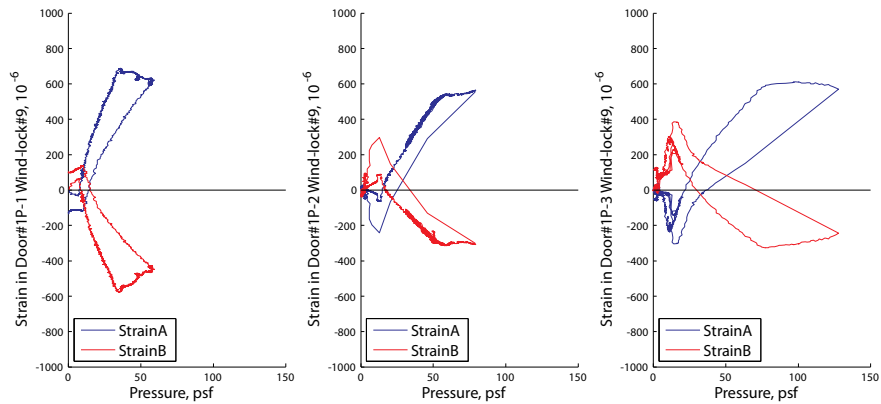
Strain in wind lock#6 in Door#1P-1 (left), Door#1P-2 (middle) and Door#1P-3(right)



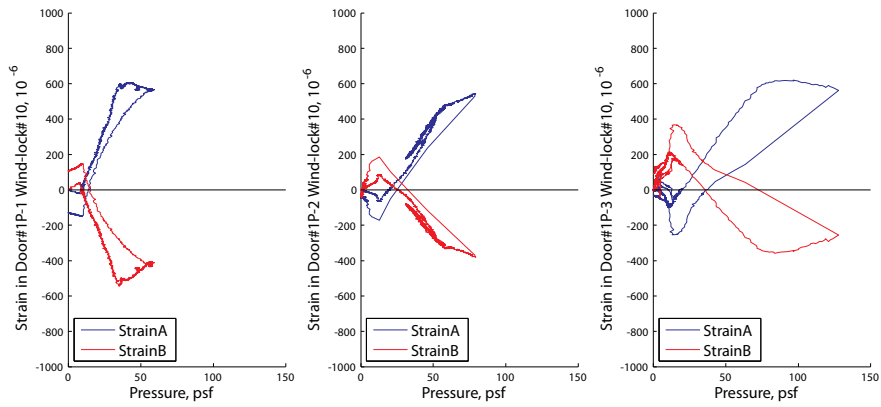
Strain in wind lock#7 in Door#1P-1 (left), Door#1P-2 (middle) and Door#1P-3(right)



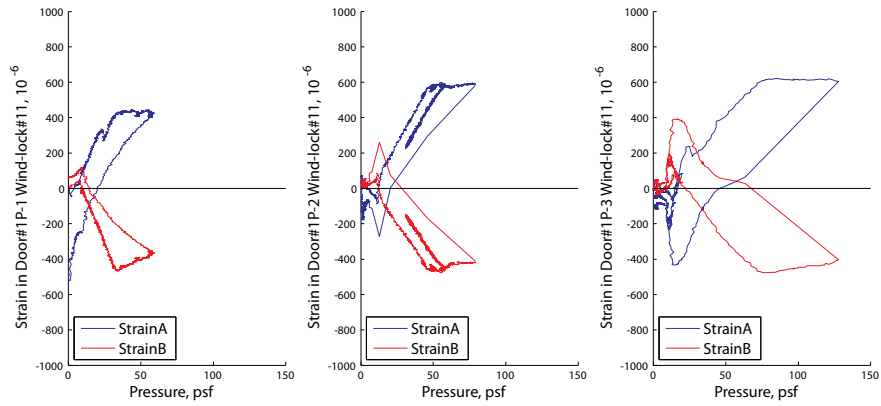
Strain in wind lock#8 in Door#1P-1 (left), Door#1P-2 (middle) and Door#1P-3(right)



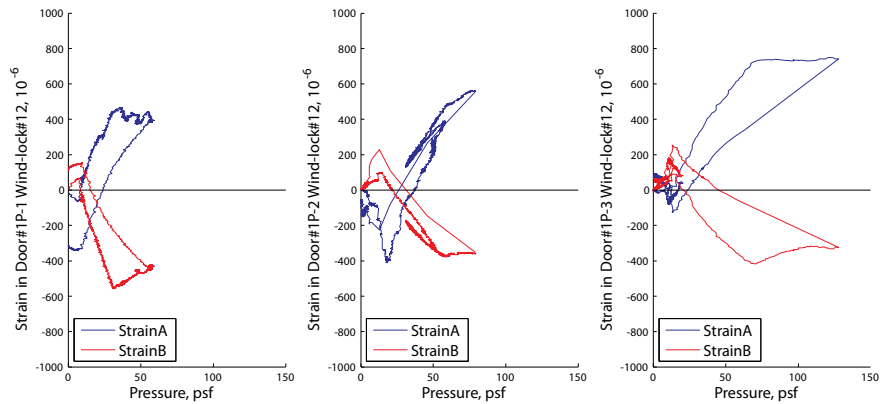
Strain in wind lock#9 in Door#1P-1 (left), Door#1P-2 (middle) and Door#1P-3(right)



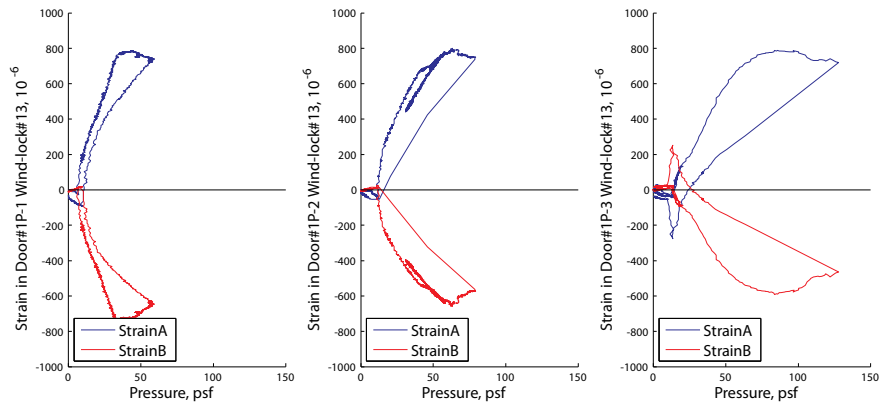
Strain in wind lock#10 in Door#1P-1 (left), Door#1P-2 (middle) and Door#1P-3(right)



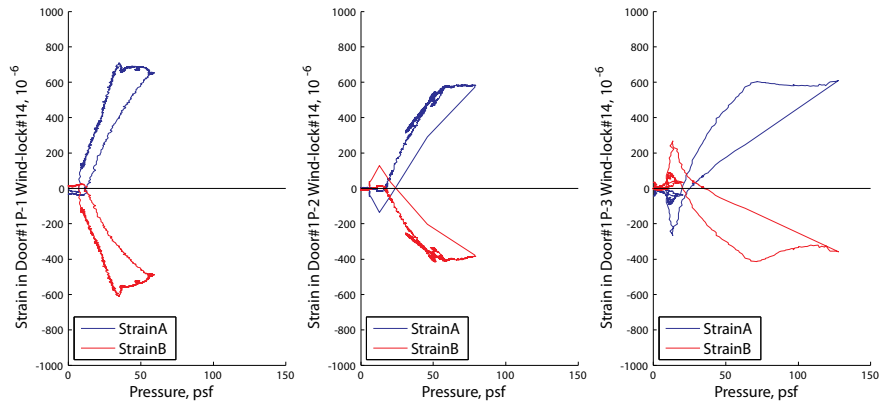
Strain in wind lock#11 in Door#1P-1 (left), Door#1P-2 (middle) and Door#1P-3(right)



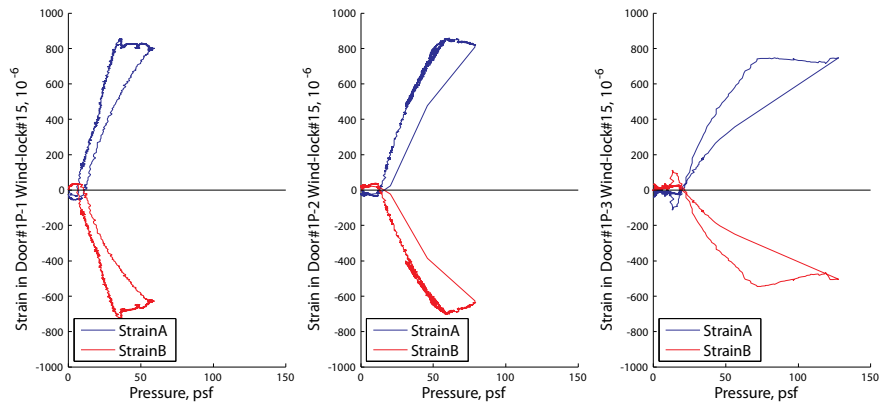
Strain in wind lock#12 in Door#1P-1 (left), Door#1P-2 (middle) and Door#1P-3(right)



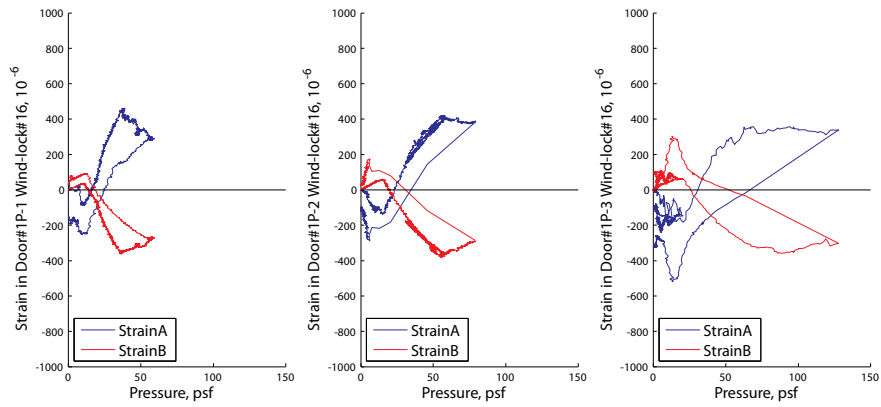
Strain in wind lock#13 in Door#1P-1 (left), Door#1P-2 (middle) and Door#1P-3(right)



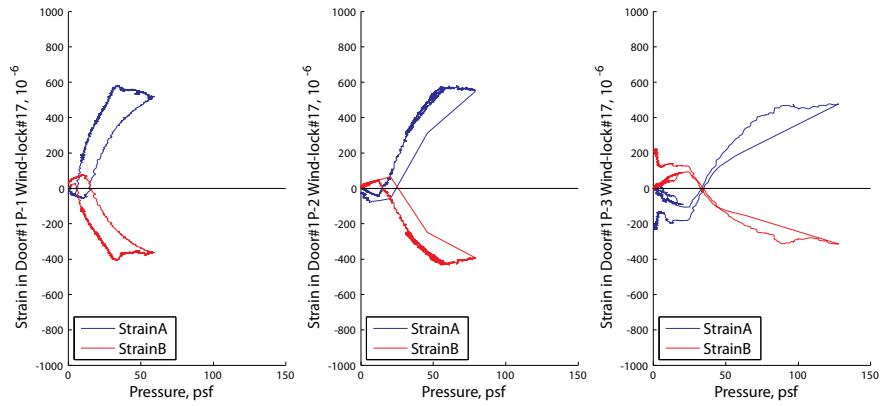
Strain in wind lock#14 in Door#1P-1 (left), Door#1P-2 (middle) and Door#1P-3(right)



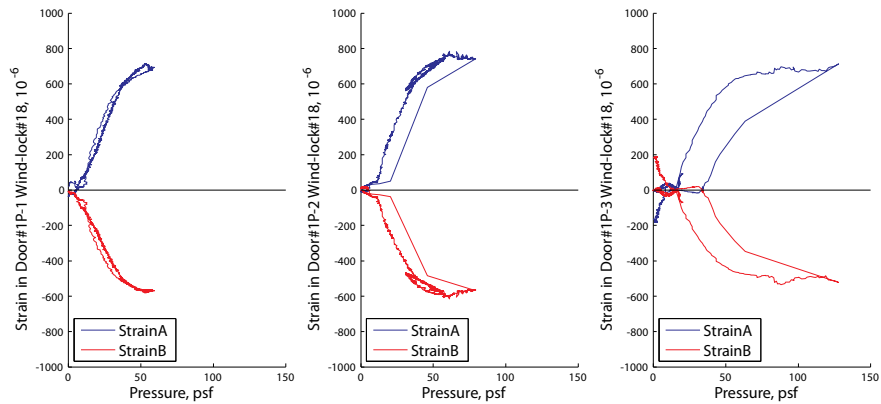
Strain in wind lock#15 in Door#1P-1 (left), Door#1P-2 (middle) and Door#1P-3(right)



Strain in wind lock#16 in Door#1P-1 (left), Door#1P-2 (middle) and Door#1P-3(right)



Strain in wind lock#17 in Door#1P-1 (left), Door#1P-2 (middle) and Door#1P-3(right)



Strain in wind lock#18 in Door#1P-1 (left), Door#1P-2 (middle) and Door#1P-3(right)